

## Quantifying the Influence of Building Rear Setbacks Geometry on Thermal and Energy Performance of Residential Buildings in Hot Arid Regions

Asmaa Omar <sup>a</sup>, Ayman Ragab <sup>a\*</sup>

<sup>a</sup> Department of Architecture Engineering, Faculty of Engineering, Aswan University, Aswan, Egypt.

### Abstract

This study investigates the impact of the aspect ratio of rear setbacks on the microclimate and energy performance of adjacent residential buildings in Aswan, Egypt's hot, arid climate. The research employs a two-phase methodology, combining field measurements and computational simulations using ENVI-met and Design Builder. The study examines how different aspect ratios (1.5, 1.87, and 2.25) influence local microclimatic conditions in the rear setback zones and adjacent indoor spaces. The findings reveal that higher height-to-width ratios reduce solar exposure, improving thermal comfort within the setback areas. Middle floors particularly benefit from enhanced natural ventilation and lower temperatures as the aspect ratio increases, with the second floor showing the greatest temperature reduction of 4.5°C between indoor and outdoor spaces. Conversely, lower floors face higher temperatures due to increased ground radiation, heat accumulation, and limited airflow, especially in regions with high solar angles. Regarding energy performance, increasing the setback ratio has a different effect on each floor level. Lower floors experience higher energy consumption due to greater heat buildup, while middle floors benefit from reduced energy demand because of improved ventilation. However, upper floors face greater solar exposure, increasing cooling needs and energy use. These findings highlight the importance of considering urban architectural elements in building design to optimize thermal comfort and energy efficiency, underscoring the connection between external microclimates and indoor energy consumption.

**Keywords:** Microclimate; Courtyard; Cooling energy; Aspect ratio; Building envelope.

### Abbreviations:

Name	Abbriviation	Name	Abbriviation
Air temperature	Ta	Universal Thermal Climate Index	UTCI
Operative temperature	To	physiologically equivalent temperature	PET
Relative humidity	RH	Mean radiant temperature	T <sub>mrt</sub>
Predicted Mean Vote	PMV	Sky view factor	SVF
Outdoor thermal comfort	OTC	Urban Heat Island	UHI

\*Corresponding author E-mail: [ayman.ragab@aswu.edu.eg](mailto:ayman.ragab@aswu.edu.eg)

Received October 18, 2024, received in revised form, November 28, 2024, accepted November 28, 2024.

## Introduction

The energy problem has many faces. Many countries feel it is vital to their national security to have access to clean, affordable energy that is linked to their economic prosperity. Globally, buildings are responsible for approximately 40% of the world's annual energy consumption. Most of this energy is used for lighting, heating, cooling, and air conditioning [1]. Energy is becoming increasingly important globally. Despite growing demand in developing countries, developed countries still consume large amounts of energy [2]. Growing populations and improvements in living conditions in many developing countries will increase energy demand. Energy consumption is highest in the most populous countries [3, 4]. On the local level, energy consumption in buildings has been receiving increasing attention in Egypt since the repeated nationwide power outages in 2012 [5, 6]. In addition, it represents more than 42% of energy consumption in Egypt [7]. Energy consumption in residential buildings in Egypt has increased significantly as people's demand for daily thermal comfort continues to grow.

In this context, it is essential to understand the various factors that influence the energy required for cooling in buildings. These factors can be broadly categorized into two primary categories. The first category encompasses the direct factors that influence the energy consumption for heating and cooling in buildings, such as building orientation [8], building shape [9], and the building envelope [10-13]. These factors have been extensively studied across various climatic regions [14]. The second category includes the indirect factors that affect building energy demand, such as the impact of urban microclimate. Urban geometry characteristics, such as sky view factor (SVF) [15], street orientation [16], shading [17], and aspect ratio [18, 19], are among the most important factors in this category. However, there is some ambiguity in this area, as previous research has primarily focused on the direct effects of the factors in the first category on building energy consumption [20].

Moreover, addressing thermal comfort is essential for understanding energy consumption in buildings. The thermal comfort of buildings is a fundamental objective in architectural design. The thermal environment significantly influences the consumption of cooling energy, particularly in warm climates, where achieving thermal comfort represents a substantial portion of a building's overall energy use [21]. The thermal comfort of residential buildings has a significant impact on the emotional and physical state of residents. For example, high temperatures or excessive heat in your home can cause various problems (sweating, fatigue, and skin irritations). Therefore, care should be taken to ensure an acceptable and comfortable indoor climate to improve the occupants' mood, health, and well-being [22].

Many indices measure external thermal comfort. The Universal Thermal Climate Index (UTCI) is a thermal comfort index that considers factors such as air temperature, humidity, wind, radiation, and clothing to describe how the human body experiences ambient conditions. It is used as a measure of thermal comfort for outdoor conditions [23]. PET serves as an index of the human perception of temperature in different environments. PET is defined as the temperature that, in a reference environment, has the same thermal balance and skin and core temperatures as the given environment [24]. The Predicted Mean Vote (PMV), introduced by Fanger in 1970 and standardized in ISO 7730 (ISO 1994), is widely recognized as the predominant index for assessing thermal comfort

in moderate indoor environments. This index is a valuable tool for evaluating and quantifying the level of thermal comfort experienced by individuals in such settings [25]. The operative temperature ( $T_o$ ) is a key concept in thermal comfort that represents the uniform temperature within a hypothetical, perfectly black enclosure (i.e., one that absorbs all radiant energy) in which an occupant would experience the same thermal exchange through both radiation and convection as they would in the actual environment. In other words, it is an averaged measure that accounts for the combined effects of air temperature and mean radiant temperature on human comfort, reflecting the heat transferred between the occupant and their surroundings [26].

### Literature review

The aspect ratio (H/W) significantly influences thermal comfort and energy consumption in buildings by affecting natural ventilation, light distribution, and sun exposure. Research indicates that optimizing H/W can enhance thermal efficiency across various climates. Abdulsalam and Hussien [18] investigate the impact of aspect ratio on outdoor thermal comfort in a hot environment, focusing on a campus in Cairo, Egypt. Using simulation models, the research shows that an aspect ratio of 3 significantly improves thermal comfort, reducing the Mean Thermal Sensation Vote (MTSV) from 2.7 to 1.4 due to enhanced shading effects. The findings suggest that increasing aspect ratios and implementing additional shading strategies effectively improve outdoor thermal conditions. Abd Elraouf et al. [27] aimed to investigate the impact of urban geometry on outdoor thermal comfort in a hot-humid climate, specifically focusing on the aspect ratio H/W in Port Said, Egypt. The ENVI-met simulation model was used to simulate environmental parameters and Rayman was utilized to convert data into physiologically equivalent temperature PET. The results showed that an H/W of 2.5 was the most appropriate urban geometry for enhanced thermal comfort in the hot-humid climate of Port Said, Egypt. The findings further indicate that aspect ratio is the most effective factor in enhancing thermal comfort, with street orientation and building typologies also playing significant roles.

Setaih [28] evaluated the effects of multiple asymmetrical street aspect ratios on urban pedestrian microclimate and outdoor thermal comfort conditions in Madinah, Saudi Arabia. The findings indicate that a leeward gradual increase in multiple asymmetrical aspect ratios of 1– 1.3– 2.3 reduces the air temperature by 3.43 K and increases wind velocity by 169.2% (i.e., from 0.65m/s to 1.75m/s), which is recommended for enhancing urban pedestrian microclimates in low wind speed environments. A small increase in wind speed significantly improves pedestrian thermal comfort conditions, with an average measurement difference of 4.8°C in PET temperature. Nasrollahi et al. [29] investigate the impact of urban geometry and shading on pedestrians' thermal comfort in Ahvaz, Iran, a hot climate region. It uses micrometeorological measurements, questionnaire surveys, and simulations to analyze the role of urban canyons, orientation, aspect ratio, and shading on PET and mean radiant temperature ( $T_{mrt}$ ). The aspect ratio of canyons also affects thermal comfort, with a reduction in aspect ratio leading to an increase in PET.

Abdollahzadeh and Nastaran [30] evaluate the thermal performance of streets in residential zones of Liverpool, NSW, Australia, and aim to improve their comfort index by investigating urban design factors affecting outdoor thermal comfort (OTC) using computational simulation techniques. The findings reveal that street canyon orientation and aspect ratio are the most influential factors

on OTC, with street canyon orientation having the highest impact. The aspect ratio has a significant impact on OTC, accounting for 30.59% of the thermal performance of streets. Bakarman [31] found that the aspect ratios have a stabilizing effect on outdoor thermal comfort, benefiting courtyards in warm climates more than in winter, concluding that the exposure of urban surfaces to solar radiation is a function of the H/W ratio and orientation of the canyon. These factors play a dominant role in determining the quantity of incoming solar radiation received by the canyon's horizontal and vertical surfaces, thus affecting the ambient air temperature and surface temperature inside the canyon. The study shows that the H/W ratio is an influential factor that contributes to the formation of the Urban Heat Island (UHI) phenomenon, which causes outdoor thermal discomfort in hot-arid climatic zones. The results of the study can be used to inform urban planning and design strategies to mitigate the UHI effect in hot-arid cities.

Jihad and Tahiri [32] highlight the significance of outdoor thermal conditions in urban design, particularly in Morocco, where both indoor and outdoor environments impact comfort levels. The study presents specific numerical results for aspect ratio in three Moroccan climatic zones: In Errachidia, the optimal aspect ratio is less than 1.2; in Agadir, the recommended aspect ratio is between 2.5 and 3.4; and in Fez, a suitable aspect ratio falls between 1.2 and 1.9. The research also suggests that higher aspect ratio canyons can still achieve comfortable climates if they incorporate historically thick walls with high thermal capacity to mitigate heat effects. Ali and Mayer [33] evaluate street design, particularly aspect ratio and solar orientation, which influence pedestrian thermal comfort in hot and dry climates, using a three-dimensional model to assess comfort via the PET. The results indicate that increasing the aspect ratio generally enhances thermal comfort, but this improvement is limited, especially for E-W-oriented streets, where even high aspect ratios still result in PET values above comfort levels. In contrast, N-S-oriented streets experience less heat stress. Notably, streets with an aspect ratio of 4 can reach maximum PET values of approximately 54°C, highlighting extreme discomfort.

Cui et al. [34] examine the impact of street design on the Urban Heat Island (UHI) effect and energy consumption, using Harbin as a case study. It highlights the influence of street ratios and vegetation on urban temperatures and energy use, emphasizing the role of street design in urban heat management. The study revealed that areas with higher street aspect ratios (greater than 1:1) experienced temperature increases of up to 3°C compared to areas with lower aspect ratios (less than 1:1). Additionally, energy consumption for cooling in these high aspect ratio areas was approximately 15% higher than in areas with more balanced street designs. Rao et al. [35] emphasize the importance of analyzing urban geometry impacts across diverse climate zones, particularly in countries like China, to develop effective climate adaptation policies. The study reveals that aspect ratio (H/W) significantly affects thermal comfort, especially in high-latitude cities. For example, Harbin experiences a maximum PET difference of 8.62°C due to H/W, Urumqi shows a 4.37°C difference, Xining 3.29°C, Xi'an 1.29°C, Kunming 0.76°C, Changsha 0.61°C, and Guangzhou 0.63°C. These findings suggest that higher H/W ratios should be adopted in high-latitude cities for better thermal comfort, while cities below 30° latitude may not need to prioritize H/W impacts.

The existing literature emphasizes the critical role of urban geometry and design in influencing thermal comfort and energy consumption in various climates. Despite the existing body of research on thermal comfort and energy efficiency, there remains a significant gap in understanding how specific architectural elements, particularly rear setbacks, influence these factors in hot, arid climates such as Aswan. This study aims to address the lack of research on the impact of rear setbacks on thermal comfort and energy performance in hot, arid regions like Aswan. Egyptian Law No. 119 of 2008, commonly called the Unified Building Law, exclusively governs planning and construction activities in Egypt. This legislation and its accompanying executive regulations incorporate various provisions about setbacks delineated using distinct terms and definitions. Specifically, setbacks are categorized into three types: frontal setback, side setback, and rear setback, each denoting the prescribed distance between the property line and the construction line in all spatial orientations [36]. Many studies have investigated how the street width ratio to building height and the dimensions of other urban spaces impact thermal comfort in the street [30, 34, 37, 38]. There is a significant research gap concerning thermal comfort within rear setbacks and their influence on indoor thermal comfort. Most existing studies have focused primarily on street ratios, with limited attention given to the minimum ratios achievable in setback areas. Additionally, these studies often concentrate solely on the impact of outdoor microclimate on the first floor, neglecting the effects on other floors of the building. So, this study seeks to examine the accurate microclimate conditions for each floor that affect the adjacent spaces and residential units in terms of thermal and energy performance. The main objective of this study is to enhance thermal comfort in rear setback areas while improving indoor thermal conditions and energy efficiency for buildings adjacent to these spaces, especially in hot climates like that of Aswan City.

## Materials and Methods

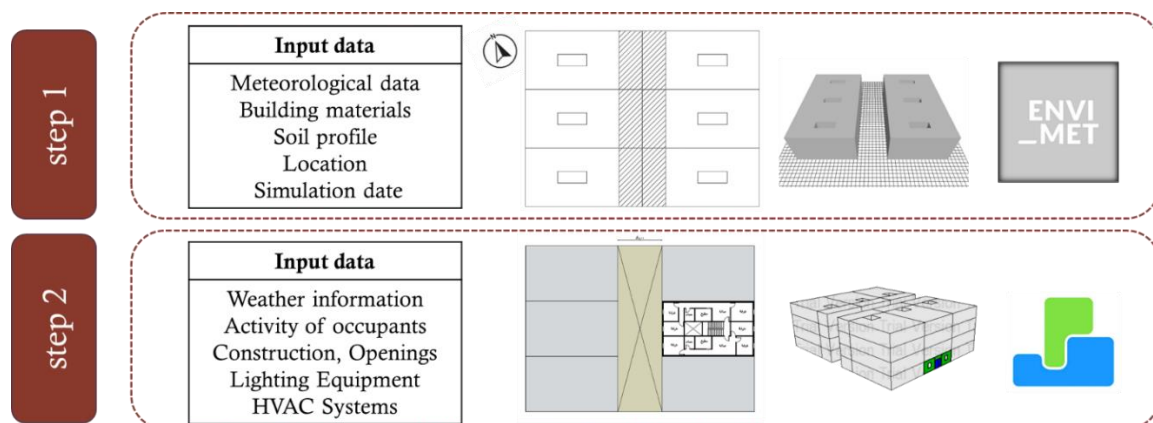


**Figure 1. The general study framework.**

In more detail, the initial phase of the study involved a comprehensive analysis of the impact of aspect ratio on external thermal performance within the rear setback across three cases: C1, C2, and C3, with aspect ratio values of 1.5, 1.87, and 2.25, respectively. To accomplish this, an experimental approach was adopted, involving field measurements of air temperature and relative humidity. Additionally, numerical simulations of the urban microclimate within the rear setbacks were carried out using ENVI-met V5.5.1 software. ENVI-met is a widely utilized computational fluid dynamics (CFD) modeling software that offers a user-friendly interface and is commonly employed by various stakeholders and researchers in disciplines related to the urban environment, such as

urban planning, landscape architecture, civil engineering, and urban climate studies [39]. The underlying structure of ENVI-met is based on a microclimate fluid dynamics model specifically designed for urban settings. By leveraging Reynolds-Averaged Navier-Stokes (RANS) equations, this software facilitates the analysis of atmospheric flow and heat transfer, enabling the evaluation of crucial meteorological parameters, including air temperature ( $T_a$ ), relative humidity (RH), wind speed ( $V$ ), and mean radiant temperature ( $T_{mrt}$ ) [39].

In this study, weather data collected using the Aswan University weather station (Hobo U30) was inputted into Envi-met. The model was designed to analyze three cases, each with different aspect ratios of 1.5, 1.87, and 2.25. The results obtained from the simulations included  $T_a$ , RH,  $V$ , and  $T_{mrt}$  for each case. The base case study model with  $H/W=1.5$  was validated by conducting a comparison between the air temperature and relative humidity data obtained from numerical simulations and the corresponding measurements collected during the experimental phase. This rigorous validation process served to ensure the accuracy and reliability of the study model. The extraction of PET results with Rayman facilitated a comprehensive assessment of the thermal comfort conditions experienced by individuals within the rear setbacks, considering the unique characteristics of the studied urban microclimate. Rayman is a specialized tool specifically designed for calculating thermal comfort indices, with PET being one of the most widely employed indices [40]. Through this scientific approach, the study provides a robust structure for evaluating and understanding the thermal comfort aspects relevant to rear setback users.

The second phase of the study focused on analyzing the internal thermal conditions and evaluating the energy efficiency of the building. The primary objective was to estimate and compare the cooling energy demands with the current case. To achieve this, simulations were conducted using Design Builder software version 7.02.006, which integrates the EnergyPlus simulation engine version 9.4. The software relies on standard EnergyPlus Weather (epw) files, which contain hourly weather data to represent the local climate conditions. Once the model was prepared, additional data was inputted into Design Builder, including building materials, activities, openings, and HVAC systems. Design-Builder is a popular energy simulation software among architects and engineers for its ability to create detailed 3D building models and simulate energy performance under various conditions. With comprehensive features such as HVAC, lighting, and renewable energy modeling, it enables accurate assessments of energy consumption and thermal comfort. A University of Nottingham study found it highly accurate in predicting building energy performance, making it a reliable tool for optimizing designs and reducing energy use. Its user-friendly interface, pre-built templates, and intuitive functionality further enhance its value for professionals seeking sustainable building solutions[41], [42].

By employing parametric simulations and various outputs, such as the energy required for cooling purposes and indoor thermal conditions, the study provides valuable insights into the internal thermal dynamics and energy efficiency of the building through this scientific approach. It enables a comparative analysis of the cooling energy demands and other relevant performance metrics for each case, contributing to a deeper understanding of the building's energy performance and the potential impact of different design factors. After measuring the energy for a day, the energy consumption for a month can be determined by scaling the CDHs observed on a specific day and

applying it to the rest of the month. This method has also been used to calculate energy consumption for the entire year. It leads to a more accurate estimation of a building's energy performance and allows for a better evaluation of proposed cases on energy efficiency. Figure 2 presents the detailed study framework and the adopted phases.

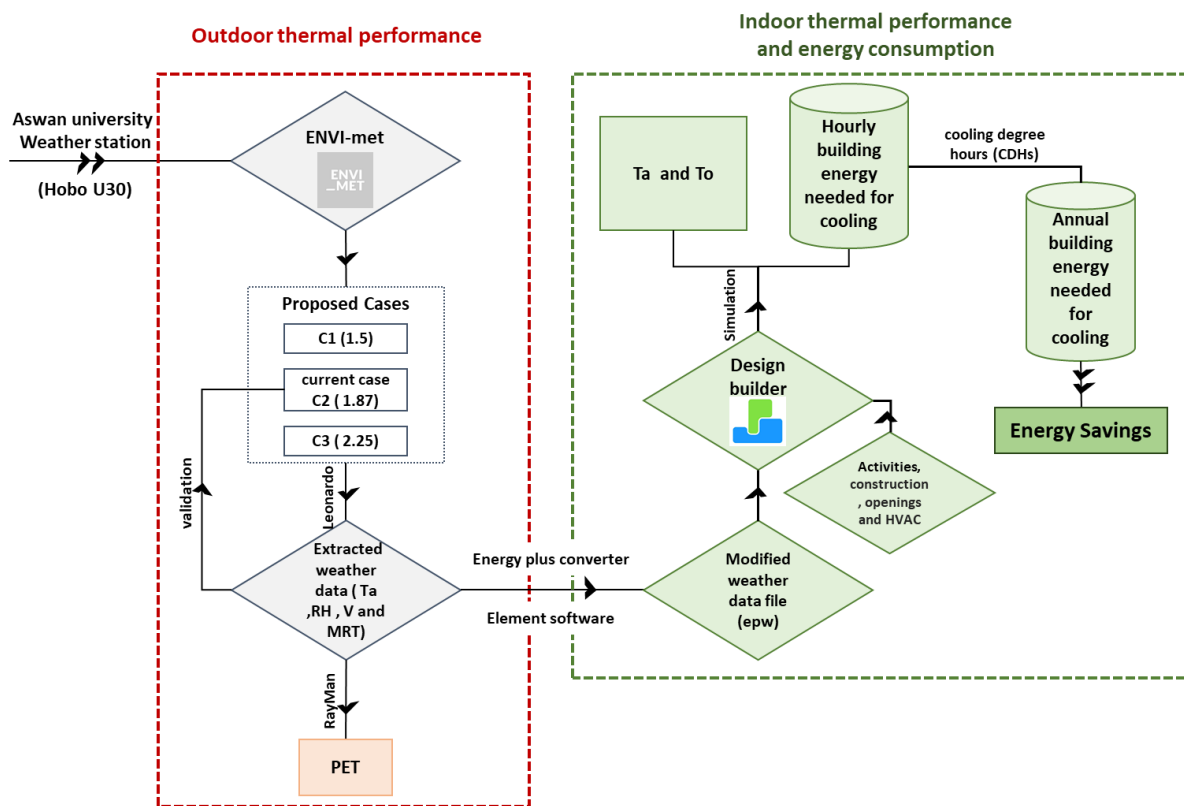


Figure 2. The detailed study framework.

### Study area and the case study model

The investigated area is Aswan City, located in southern Egypt. Aswan is geographically positioned at 24.0861° N latitude and 32.8989° E longitude, with an altitude of approximately 194 meters above sea level and is situated on the eastern bank of the Nile River. The region is characterized by a hot desert climate, with soaring temperatures throughout the year, ranging from 32°C in January to 42°C in June [43-45]. The area experiences limited precipitation, with an average of only 1mm annually. The area falls under the Köppen climate classification Zone BWh, which denotes a hot, arid climate, as shown in Figure 3.

In this study, a residential building model is used in the Al-Aqqad district of Aswan. The building chosen for the study is a five-story building with two flats per floor and an average flat area of 75m<sup>2</sup>, with a total area of approximately 160m<sup>2</sup> including the staircase space. The height of each floor is 3m, and the window-to-wall ratio is around 10%. The rear setback between the two buildings measures 8m, with each building leaving a 4-meter space between the property line and the construction line. The study concentrates on the aspect ratio rather than other factors, such as the sky view factor, as no difference in its effect is observed due to the regular shape of the rear setback. The rear setback is a semi-private space that can be used by the residents of the two buildings and is a suitable place for outdoor activities. The architectural plan of the building under investigation is illustrated in Figure 4.

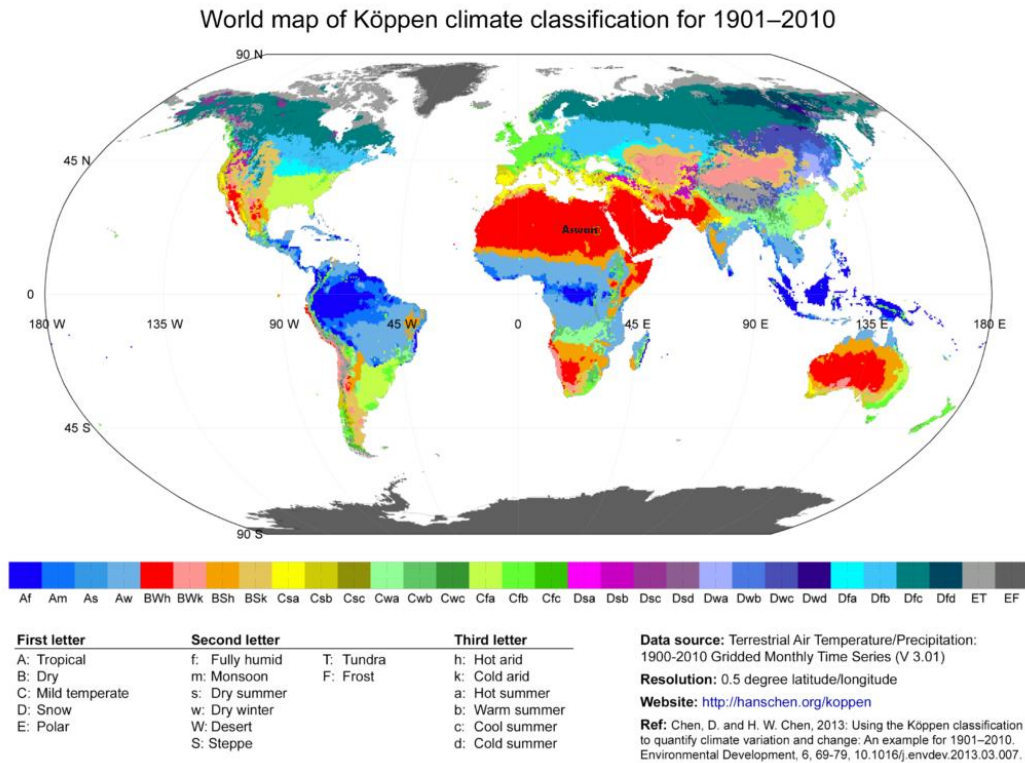


Figure 3. The Köppen climate classification.

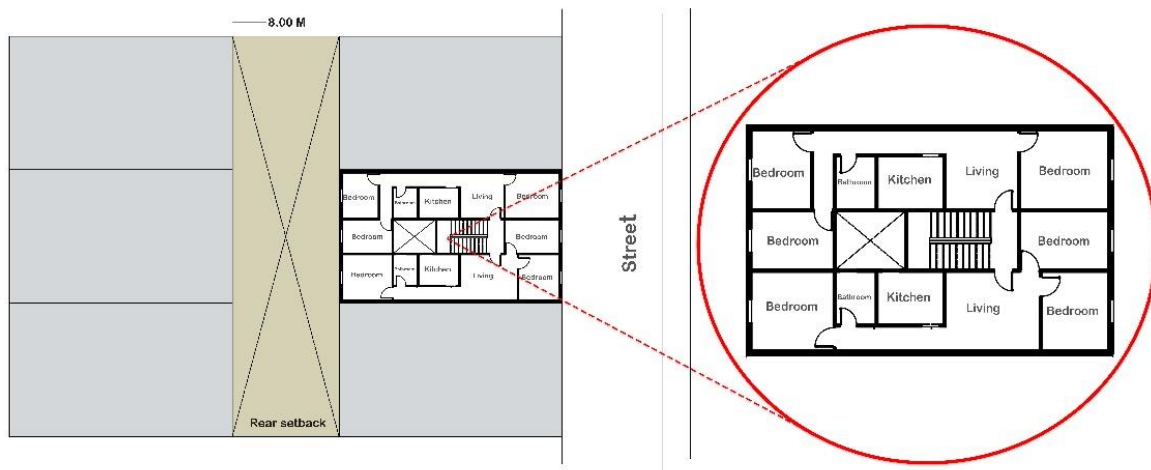
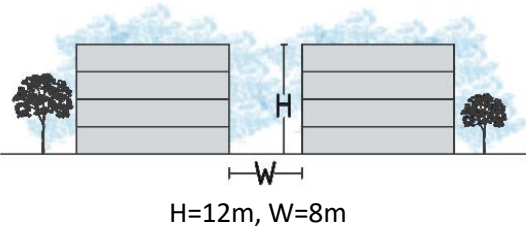
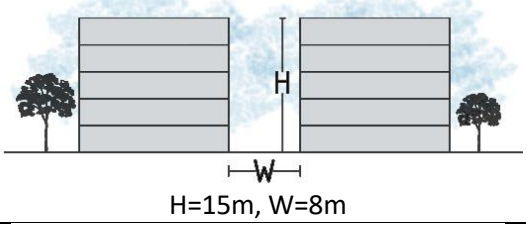
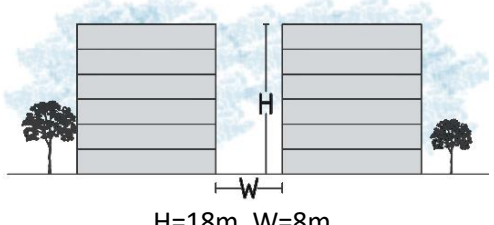


Figure 4. The architectural plan of the building under investigation

### Proposed cases in terms of aspect ratio

A study is conducted on three cases to analyze the effect of aspect ratio on thermal comfort and energy demand in a building. The investigation is conducted in the rear setback area between two buildings, with a previously presented attribute. The variable in the study is the height of each investigated building, with the first case depicting a height of 12 m and an aspect ratio (H/W) of 1.5. The current case involved a building height of 15 m with a ratio of 1.87, and the last case depicted a height of 18 m with a ratio of 2.25. These investigated cases are illustrated in Table 1.

**Table 1. The proposed aspect ratios for the rear setback.**

Abbreviations	Aspect Ratio (H/W)	Section
C1	1.5	 <p>H=12m, W=8m</p>
C2 (current case)	1.87	 <p>H=15m, W=8m</p>
C3	2.25	 <p>H=18m, W=8m</p>

## Simulation Procedure Overview

### Outdoor Simulation

The case study building was modeled as a 2-dimensional footprint in AutoCAD software, converted to a bitmap format (.bmp), and imported into the ENVI-met software. The digitization process was performed, and the meteorological inputs, which were measured using the Aswan University weather station (Hobo U30), and the building materials were completed before conducting a simulation. The ENVI-met software has a limit that extends to the extensive time required to complete simulations, making it unsuitable for year-long applications. So, it was used to simulate a specific day, namely July 2nd, 2023. By initiating the simulation four hours before the target day and extending it to a total of 28 hours, the ENVI-met model sought to account for any potential inaccuracies in the initial phase and to comprehensively analyze the environmental conditions under investigation [46]. The simulation yielded results for various parameters, including  $T_a$ , RH, V, and  $T_{mrt}$ . The study involved the implementation of simulations for three specific cases that were under investigation. The results of the measurements were systematically collected at each floor level to capture the variations and changes resulting from the investigation case.

Table 2 presents a comprehensive summary of the data inputs used in the investigated case study. The meteorological inputs, derived from the specific weather data for the study location, formed the foundation of the simulation process. In addition to the weather data, human biometeorological parameters and information about the building materials were included as crucial data inputs for the simulations.

**Table 2. Summary of data entry for the case study.**

Parameter	Value
Number of main area grid boundary	40, z = 50, y = 50x=
Soil profile for all grids	loamy soil and concrete pavement light
Grid-scale	x = 2, y = 2, z = 2
Walls material	plaster, Brick wall, plaster thickness of layers (m) = (0.02, 0.12, 0.02) Albedo = 0.4
Roof materials	Reinforced concrete thickness = 0.2 m, Albedo = 0.3
Simulation date	2nd of July
Start wind speed at 10 m height (m/s)	2
Start wind direction (°)	90 from north
Max air temperature (°C)	42.29
Min air temperature (°C)	25.80
Initial specific humidity of atmosphere (g/Kg)	8
Max relative humidity (%)	36.5
Min relative humidity (%)	14.80

Subsequently, the Rayman software was employed to examine the external thermal comfort index, specifically the PET, utilizing the results obtained from ENVI-met simulations. The ENVI-met outputs, including Ta, RH, V, and Tmrt, were utilized as inputs for the Rayman analysis. By employing Rayman, a comprehensive evaluation of the PET index, which quantifies the thermal comfort experienced by individuals in the outdoor environment in rear setbacks, was conducted. This integrated approach utilizing ENVI-met and Rayman enabled a thorough investigation of the outdoor thermal comfort of rear setbacks through proposed cases.

### **Indoor Simulation**

To assess a building's internal thermal comfort and energy demand, a simulation using Design Builder was conducted for a single day, specifically on July 2nd, 2023, which marked the hottest day of the year in Aswan [47]. The building was modeled as a 2-dimensional architecture plan in AutoCAD software and subsequently imported into Design Builder version 7.02.006. The process involved developing a simplified building model, which included assigning local properties for walls, roofs, and windows as shown in Table 3. The model incorporated comprehensive HVAC systems. In addition to HVAC systems, the model considered internal loads, including equipment, lighting, and appliances, which emit heat and contribute to the overall thermal conditions of the building. The specific characteristics and energy consumption profiles of these internal loads were considered to accurately represent the building's energy dynamics. The model incorporated activities and schedules that were tailored to the specific building type, as shown in Table 3 (b). Different building types have varying occupancy patterns, such as working hours, occupancy density, and usage intensity. By considering these factors, the model was able to simulate realistic cases that reflected the building's daily operations and occupant behavior.

**Table 3. Summary of data entry for the case study.**

Item	Specification
Building type	Residential building
Location	Aswan City—Hot desert climate (Köppen: BWh)
Floor area (m <sup>2</sup> )	160
No of Floor	C1: Ground floor and three floors C2: Ground floor and four floors C3: Ground floor and Five floors
Floor height (m)	3
Window glazing	3 mm single clear glazing
Window-to-wall ratio	10%
Window orientations	East and West
Wall cross-section	0.02 m cement plaster, 0.12 m brick, 0.02 m cement plaster
HVAC	split air conditioning for each room
Nominal power (kw)	2.23
Cooling setpoint (°C)	25
Heating setpoint (°C)	18

Weather data was entered for each case. The Aswan 2002 epw file, provided with EnergyPlus, was selected as the baseline weather data for the location. To simulate the impact of different proposed cases, a customized epw file was generated. This involved a two-step process. Firstly, the original weather data in the epw file was replaced with synthesized microclimate data. This microclimate data was obtained from the ENVI-met model results. In the second step, the Element and EnergyPlus converter software was employed to convert the ENVI-met model results into a compatible format for EnergyPlus. This conversion process ensured that the synthesized microclimate data could be incorporated into the customized epw file and used as input for the EnergyPlus simulations. By integrating the synthesized microclimate data from the ENVI-met model into the customized epw file, the model could simulate the impact of different proposed cases more accurately. The study specifically examined the impact of the thermal conditions within the setbacks on the building, excluding the influence of the street, as Design Builder permits the use of only one epw file. For each of the investigated cases, a separate simulation was performed for every individual floor of the building. This approach allowed for a detailed analysis of the impact of the investigations investigated cases on each floor level. The simulations conducted for each floor utilized the customized epw file with the EnergyPlus simulation engine.

One of the primary outputs obtained from the simulations was the energy required for cooling purposes. This metric quantified the amount of energy consumed by the HVAC systems to maintain comfortable indoor temperatures. In addition to energy consumption, the simulations also provided data on indoor thermal conditions. Key parameters such as  $T_a$ , RH, and operative temperature were monitored and analyzed.  $T_a$  represented the actual temperature within the indoor environment, while RH indicated the level of moisture in the air. On the other hand, the operative temperature quantifies the thermal comfort level experienced by occupants.

To determine the energy consumption for the entire month of July, the energy consumption output obtained through Design Builder is appropriately scaled. This scaling process involves cross-multiplying the cooling degree hours (CDHs) observed on the 2nd of July to estimate the energy

consumption for the remaining days of the month while considering the CDHs of the simulated day. Similarly, to calculate the energy consumption for the entire year, the cooling degree hours for each month are considered. Adopting this approach can achieve a more comprehensive assessment of the influence of proposed cases on the building's energy consumption. This method considers the variations in energy demand across different months, leading to a more accurate estimation of the building's overall energy performance. Scaling the energy consumption outputs using CDHs enables a more precise assessment of how the proposed cases affect energy efficiency.

### Field measurements

To validate the simulation model, experimental measurements were conducted in the rear setback areas at a central location throughout the day. The primary objective was to compare the results of the outdoor simulation with those of the field measurements. The measurements were taken on July 2, 2023, at the beginning of each hour. Air temperature and relative humidity were recorded at a height of 1.5 m in the center of the rear setback space. A "HOBO U12" data logger was used, positioned inside customized solar radiation shields to ensure accurate readings and minimize the influence of direct sunlight as shown in Figure 5 [48]. The measuring instrument was programmed to capture air temperature and relative humidity at one-hour intervals for 24 hours. The Specifications of the used device "HOBO U12" data logger have been presented in Table 4 [49].

**Table 4. Specifications of a "HOBO U12" data logger [49].**

Measurement range	Temperature: -20° to 70°C (-4° to 158°F) RH: 5% to 95% RH
Accuracy	Temperature: $\pm 0.35^{\circ}\text{C}$ from 0° to 50°C; RH: $\pm 2.5\%$ from 10% to 90%.
Resolution	Temperature: 0.03°C at 25°C; RH: 0.03% RH
Weight	46 g
Dimensions	58 x 74 x 22 mm

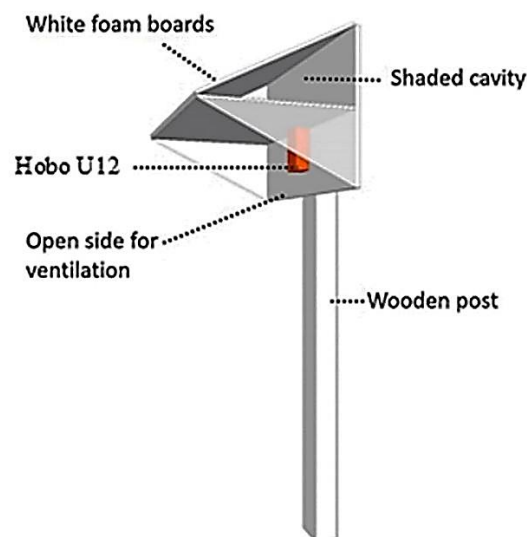


**Figure 5. Installation of the HOBO U12 device in the field.**

### Verifying the Accuracy of the Study Model

A rigorous verification process was conducted to verify the ENVI-met model in replicating microclimate conditions by comparing the simulated air temperature and relative humidity values

with the observed data in the rear setbacks on the previously mentioned day. To ensure robust validation, the verification spanned a comprehensive timeframe from 12:00 a.m. to 11:00 p.m. the following day. The agreement between the simulated and recorded values was assessed using matching coefficients to determine the level of concordance. The coefficient of determination ( $R^2$ ) was employed as a metric to quantify the strength of the association between the simulated and observed values. Notably, a high level of agreement was observed for both air temperature and relative humidity, with  $R^2$  values of 0.9299 and 0.9863, respectively. Visual representations of these results can be seen in Figures 6 (a) and 6 (b).  $R^2$  value greater than 0.75 indicates a strong correlation. Additionally, the RMSE value falls within the acceptable range of  $\pm 30\%$  for hourly data [50]. The RMSE values for air temperature and relative humidity were observed, with RMSE values of 1.74 and 0.97, respectively.

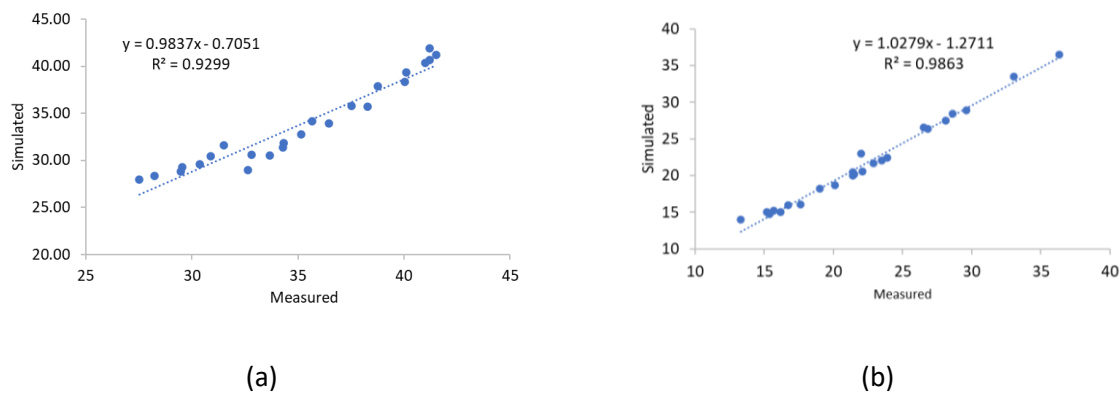


Figure 6. Validation of the study model in terms of (a) air temperature; and (b) relative humidity.

In the second phase, the energy model has been validated. The validation of the simulation model was performed by comparing the measured and simulated monthly energy consumption data, as presented in Figure 7 (a) and (b). A linear regression analysis yielded the equation ( $y = 1.2906x - 124.99$ ) with a coefficient of determination  $R^2$  of 0.989, indicating an excellent correlation between measured and simulated values. This high  $R^2$  reflects the model's ability to accurately capture energy consumption patterns, with minimal deviations observed during peak consumption months (June–August). The regression results demonstrate a strong linear relationship and confirm the reliability of the simulation model for predicting energy performance. These findings validate the model's suitability for evaluating energy efficiency and optimizing building performance in similar contexts.

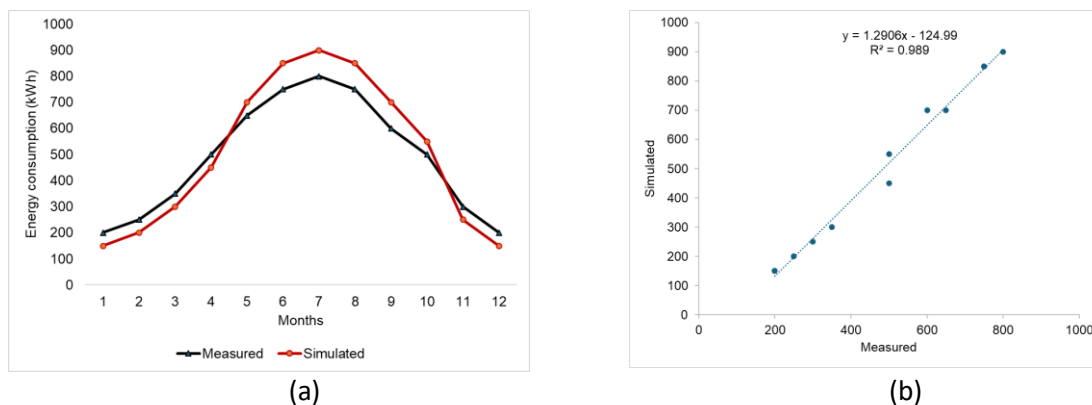


Figure 7. Energy model validation, (a) Comparison between the measured and simulated data, (b) The linear regression.

## Scope and limitations

The scope and limitations of a study assessing building performance within a defined context. Spatially, the study focuses on a residential building in Aswan's hot arid climate, specifically within the rear setback area. Temporally, the analysis is confined to the year 2023, offering insights into building performance over a single year. Qualitatively, the study considers the building's aspect ratio as a significant variable influencing outcomes. However, there are limitations. The spatial scope excludes other climatic regions and urban configurations, which may restrict the generalizability of the results. Temporally, the study does not incorporate future climate change scenarios. Qualitatively, it does not explore alternative mitigation strategies, focusing solely on the chosen approach. This clearly defined scope and limitations provide structure to the study while acknowledging the constraints that may affect the wider applicability of its findings.

## Results and discussion

### Rear setback thermal performance

#### *Analysis of Air Temperature and Relative Humidity Profiles*

Table 5 provides an in-depth analysis of temperature fluctuations in the rear setback area and adjacent rooms. Temperature and humidity readings for the middle room, collected across various floors using the Design-Builder, were utilized as a representative measure of the average thermal conditions on each floor. Temperatures were recorded at different floor levels, capturing external and internal temperatures and their respective variations. Negative temperature differences ( $\Delta T$ ) indicate indoor temperatures exceeding outdoor ones, while positive values suggest the opposite. The most significant positive  $\Delta T$  in terms of maximum temperature, indicating the largest temperature difference, was recorded on the second floor of C2, showing a notable 4.5°C difference between indoor and outdoor temperatures. Additionally, the rise in outdoor temperatures with increased height is due to greater exposure to direct sunlight, reduced shading, and the stack effect, where warm air rises and accumulates at higher levels. Interior temperatures varied across floors, with a noticeable trend of temperature increases on upper floors across all scenarios, suggesting that internal temperatures tend to rise with elevation. On the ground floor (GF), there were subtle temperature discrepancies across the proposed cases. The average outdoor temperature was consistent across all cases, equal for C2 and C3. At the same time, the highest and lowest values were closely matched in both C1 and C2, but C3 is the highest at internal temperatures. Moving to the 1st floor, C1 exhibited the highest recorded temperature, with temperatures relatively close among the different cases. The 2nd floor showcased the lowest internal temperature and the most significant improvement between internal and external temperatures in C2, with results similar across cases. On the 3rd floor, temperatures were comparable among the cases, with C1 recording the highest temperatures as it represents the topmost floor. For the 4th floor, a comparison was conducted between C2 and C3, with C2 recording the highest temperature as it is positioned as the topmost floor within its respective case. Finally, on the fifth floor, only C3 remained, recording the highest temperature as it represents the topmost floor in this case.

**Table 5. Temperature analysis across different floors and proposed cases**

Floors	Proposed cases	T <sub>a</sub> min (°C)			T <sub>a</sub> max (°C)			T <sub>a</sub> avg (°C)		
		Outdoor	Indoor	ΔT	Outdoor	Indoor	ΔT	Outdoor	Indoor	ΔT
GF	C1	27.48	35.29	-7.81	41.49	38.45	3.04	35.08	36.98	-1.9
	C2	27.53	35.28	-7.75	41.5	38.42	3.08	35.04	36.95	-1.91
	C3	27.68	35.67	-7.99	41.34	38.98	2.36	35.04	37.38	-2.34
1st	C1	27.52	35.08	-7.56	41.76	38.49	3.27	35.07	36.95	-1.88
	C2	27.75	36.22	-8.47	41.39	39.49	1.9	35.08	38.03	-2.95
	C3	27.91	36.23	-8.32	41.24	39.44	1.8	35.08	37.99	-2.91
2 <sup>nd</sup>	C1	27.98	36.38	-8.40	41.28	39.87	1.41	35.14	38.25	-3.11
	C2	27.99	33.38	-5.39	41.15	36.64	4.51	35.11	35.19	-0.08
	C3	28.03	36.15	-8.12	41.08	39.35	1.72	35.1	37.92	-2.82
3 <sup>rd</sup>	C1	28.31	41.08	-12.77	41	46.16	-5.16	35.18	43.51	-8.33
	C2	28.27	36.33	-8.06	41.01	39.74	1.27	35.13	38.17	-3.04
	C3	28.32	36.18	-7.86	40.94	39.38	1.56	35.12	37.93	-2.81
4 <sup>th</sup>	C2	28.47	41.15	-12.68	40.86	46.19	-5.33	35.15	43.55	-8.4
	C3	28.49	36.3	-7.81	40.78	39.67	1.11	35.14	38.11	-2.97
5 <sup>th</sup>	C3	28.47	41.013	-12.54	40.85	45.95	-5.1	35.15	43.37	-8.22

The simulations revealed significant daily fluctuations in air temperature. Specifically, the air temperature showed a rise from 6:00 a.m., reaching its peak at 2:00 p.m., and subsequently undergoing a gradual decline throughout the afternoon and evening. Conversely, indoor temperatures surpassed outdoor temperatures from 6:00 p.m. to 9:00 a.m., with indoor temperatures remaining lower than outdoor temperatures for the rest of the day. However, this trend varied across the upper floors in (C1, C2, and C3); indoor temperatures remained higher than outdoor temperatures throughout the day, as depicted in Figure 8. The external temperatures demonstrate convergence, while the internal temperatures exhibit distinct patterns on each floor. On GF Figure 8 (GF), C3's internal temperature rises steadily throughout the day, converging between C1 and C2. Moving to the 1st floor (Figure 8 (1<sup>st</sup>)), C1 registers the lowest internal temperature, while convergence occurs between C2 and C3. On the 2nd floor (Figure 8 (2<sup>nd</sup>)), C2 maintains the lowest temperature and shows the most significant improvement. C1's temperature surpasses that of C3. The 3rd floor (Figure 8 (3<sup>rd</sup>)) sees C1 with the highest temperature throughout the day. Transitioning to the 4th floor (Figure 8 (4<sup>th</sup>)) after C1, the comparison is between C2 and C3, with C2 recording the higher temperature. On the 5th floor, only C3's temperatures are recorded (Figure 8 (5<sup>th</sup>)), with internal temperatures consistently higher than external ones throughout the day. During the night, the building retains more heat than the surrounding environment, resulting in indoor temperatures remaining higher than outdoor temperatures until early morning. This pattern is not uniform across all floors. The upper floors consistently exhibit indoor temperatures exceeding outdoor temperatures throughout the day. The simulations also highlight a diurnal pattern in temperature fluctuations, with peaks in the afternoon around 2:00 p.m. and gradual cooling throughout the evening. This pattern aligns with typical solar heating dynamics, where

surfaces absorb heat during the day and release it as temperatures drop. Interestingly, the study notes that indoor temperatures are consistently higher than outdoor temperatures on the upper floors throughout the day, suggesting that heat retention or solar gain on these floors is a significant factor. This finding is particularly evident in scenario C1, where the highest temperatures were recorded on the 3rd and 4th floors, possibly due to less effective insulation or increased solar exposure.

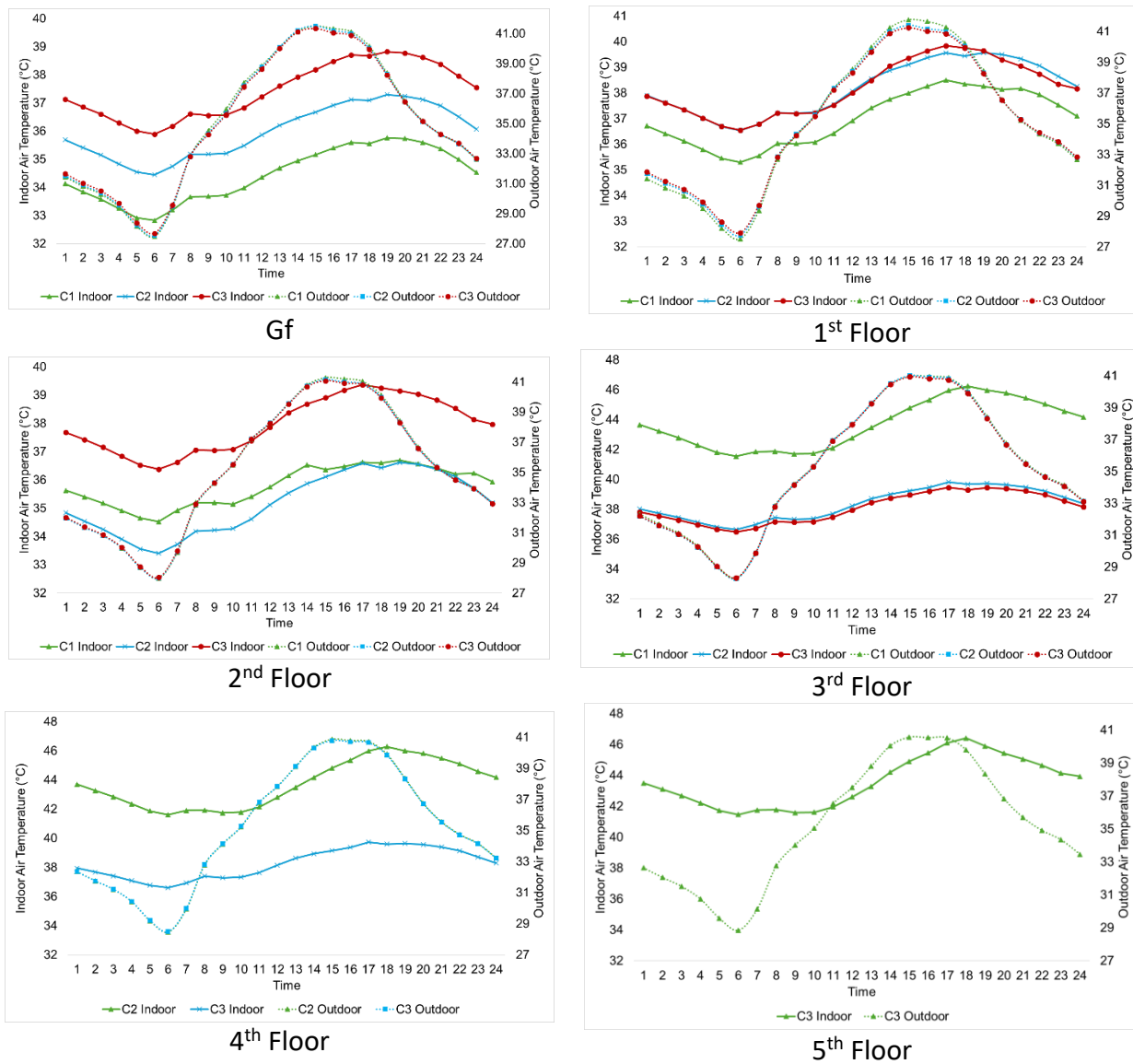


**Figure 8. Examine the temperature trends throughout the day across various cases.**

Table 6 provides a detailed analysis of an in-depth simulation study that meticulously examined the distribution of microclimatic air temperatures within a rear setback area. Measurements were taken at a height of 1.4 meters to ensure precision in capturing thermal exposure to meet the pedestrian level. Temperature data was recorded at specific intervals during peak summertime conditions, notably at 10 a.m., 12 p.m., 2 p.m., 4 p.m., and 6 p.m., offering a detailed profile of heat distribution over diurnal cycles, as outlined in Table 4. The simulation outcomes provided a comprehensive mapping of temperature variations under local solar geometry. The primary aim of this analysis was to characterize both the fundamental patterns of heat intensity and the alterations induced by the aspect ratio. Through examination of the simulation results, notable daily fluctuations

in air temperature within the rear setback area were discerned. Specifically, temperatures exhibited a trajectory of ascending from 6 a.m. to peak at 2 p.m. This can be attributed to the sun's high angle during that hour, followed by a gradual decline throughout the afternoon and evening, with temperatures spanning from 27 °C to 41.5 °C.

**Table 6. Analyzing thermal diagrams in the rear setback**

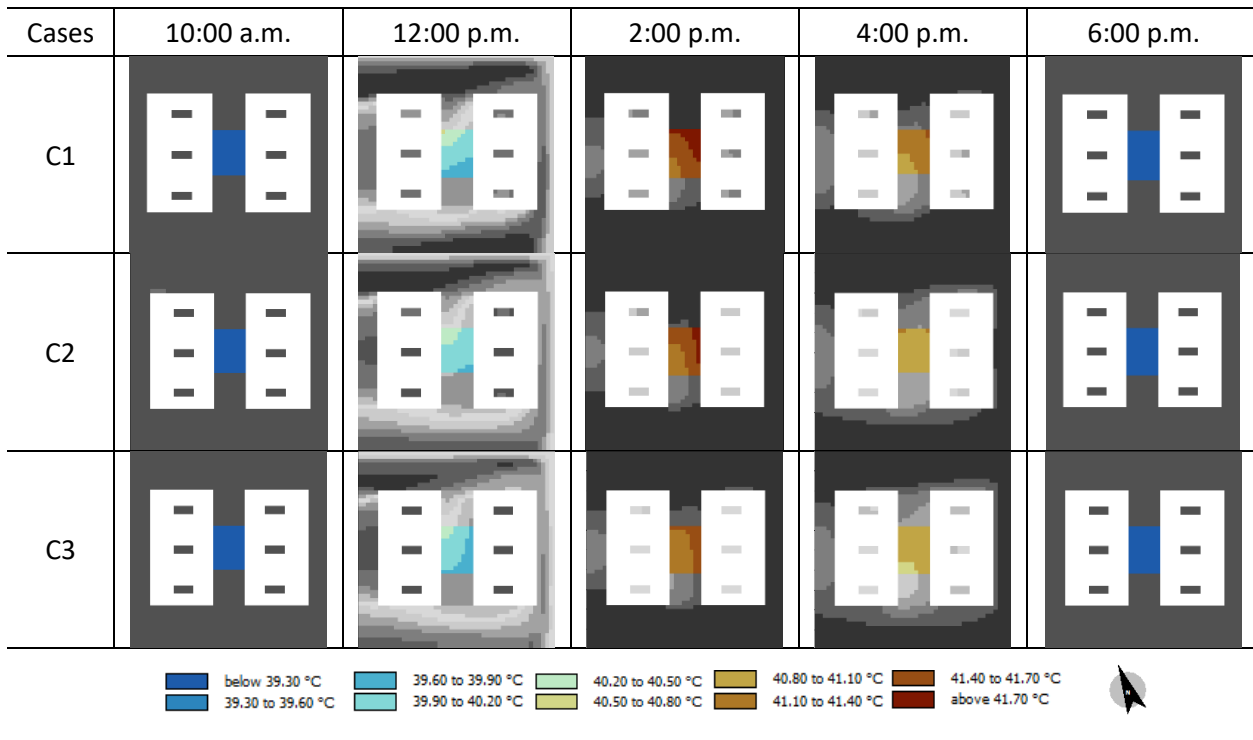


Table 7 presents an analysis of relative humidity data collected from indoor and outdoor settings across various floors and proposed scenarios. A significant variation in relative humidity levels between indoor and outdoor settings across different cases and floors was observed. Most values in the table are low due to high temperatures. The highest relative humidity value was noted on the second floor of scenario C2. Additionally, indoor relative humidity varied across floors, with a significant trend of decreasing relative humidity on higher floors across all scenarios, indicating an inclination of indoor relative humidity towards decreasing with elevation. On the GF, slight differences in relative humidity were observed across proposed scenarios. The average outdoor relative humidity remained close in all cases, while the highest and lowest values closely matched both C1 and C2, but C3 exhibited the lowest indoor relative humidity. Moving to the 1st floor, C1 showed the highest recorded relative humidity, followed by C2 and C3. The 2nd floor exhibited the highest relative humidity value and the most significant improvement between indoor and outdoor relative humidity in C2, followed by C3, and then C1. On the 3rd floor, relative humidity values were similar in most cases, with C1 recording the lowest indoor relative humidity as it represents the upper floor. Concerning the 4th floor, a comparison between C2 and C3 revealed that C2 recorded the lowest relative humidity values as it is located on the upper floor within its enclosure. Finally, on the 5th floor, only C3 remained, recording the lowest relative humidity value as it represents the upper floor in this scenario. The observed variations in relative humidity levels underscore the influence of both internal and external factors, including floor elevation and scenario-specific conditions. The

trend of decreasing indoor relative humidity with increasing elevation aligns with expectations based on natural ventilation and moisture distribution.

**Table 7. Relative Humidity Analysis across Different Floors and Proposed Cases**

Floors	Proposed cases	RH min (%)			RH max (%)			RH avg (%)		
		Outdoor	Indoor	ΔT	Outdoor	Indoor	ΔT	Outdoor	Indoor	ΔT
GF	C1	15.06	17.19	-2.13	32.6	23.18	9.42	21.77	19.82	1.95
	C2	15.1	17.16	-2.06	32.52	23.2	9.32	21.79	19.77	2.02
	C3	15.19	16.62	-1.43	32.2	22.67	9.53	21.75	19.38	2.37
1st	C1	14.82	17.21	-2.384	32.5	23.14	9.36	21.81	19.76	2.05
	C2	15.14	16.1	-0.96	32.03	21.95	10.08	21.71	18.72	2.99
	C3	15.25	16.14	-0.89	31.69	21.73	9.96	21.69	18.67	3.02
2 <sup>nd</sup>	C1	15.19	15.1	0.09	31.49	21.56	9.93	21.63	18.48	3.15
	C2	15.3	18.92	-3.62	31.5	25.15	6.35	21.65	21.67	-0.02
	C3	15.33	16.22	-0.89	31.45	21.8	9.65	21.63	18.74	2.89
3 <sup>rd</sup>	C1	15.4	11.68	3.72	30.8	16.87	13.93	21.55	14.1	7.452
	C2	15.39	16.12	-0.73	30.9	21.87	9.03	21.59	18.58	3.01
	C3	15.44	16.31	-0.87	30.8	22.09	8.71	21.59	18.81	2.78
4 <sup>th</sup>	C2	15.52	11.66	3.86	30.48	16.56	13.92	21.54	14	7.55
	C3	15.56	16.18	-0.62	30.45	21.63	8.82	21.54	18.58	2.96
5 <sup>th</sup>	C3	15.72	11.77	3.95	29.81	16.91	12.9	21.48	14.19	7.29

-3.70% 11.6% 14% 32.6%

The simulations revealed significant daily fluctuations in relative humidity. Specifically, relative humidity decreased starting at 6:00 a.m., reaching its lowest point at 2:00 p.m., then gradually increased throughout the afternoon and evening. Indoor relative humidity exceeded outdoor relative humidity from 11:00 a.m. to 5:00 p.m., with indoor relative humidity remaining lower than outdoor relative humidity for the rest of the day. However, this trend varied across the upper floors in C1, C2, and C3, where indoor relative humidity remained lower than outdoor relative humidity throughout the day, as illustrated in Figure 9. External relative humidity demonstrated convergence, while internal relative humidity exhibited distinct patterns on each floor. On GF (Figure 9 (GF)), the internal relative humidity in C3 decreased consistently throughout the day, converging between C1 and C2. Moving to the 1st floor (Figure 9 (1<sup>st</sup>)), C1 recorded the highest internal relative humidity, while convergence occurred between C2 and C3. On the 2nd floor (Figure 9 (2<sup>nd</sup>)), C2 maintained the highest relative humidity and showed the most significant improvement. The relative humidity in C3 surpassed that of C1. The 3rd floor (Figure 9 (3<sup>rd</sup>)) showed C1 with the lowest relative humidity throughout the day. Transitioning to the 4th floor (Figure 9 (4<sup>th</sup>)), after C1, the comparison was between C2 and C3, with C2 recording lower relative humidity. On the 5<sup>th</sup> floor, only relative humidity of C3 was recorded (Figure 9 (5<sup>th</sup>)), with internal relative humidity consistently lower than external relative humidity throughout the day. RH levels decreased with elevation, likely due to the reduction in moisture content as air rises and heats up. The highest RH was on the second floor of scenario C2, which also showed the largest temperature difference, suggesting that scenario C2 might have higher moisture retention or less effective moisture dispersion. The consistent decrease in RH on higher

floors reflects natural ventilation patterns where warm, moisture-laden air rises and disperses, leaving lower RH at upper elevations. Scenario C3, which had the lowest indoor RH, may benefit from better ventilation or reduced moisture intrusion. Overall, the observed RH trends highlight the influence of building design and temperature on internal moisture levels.

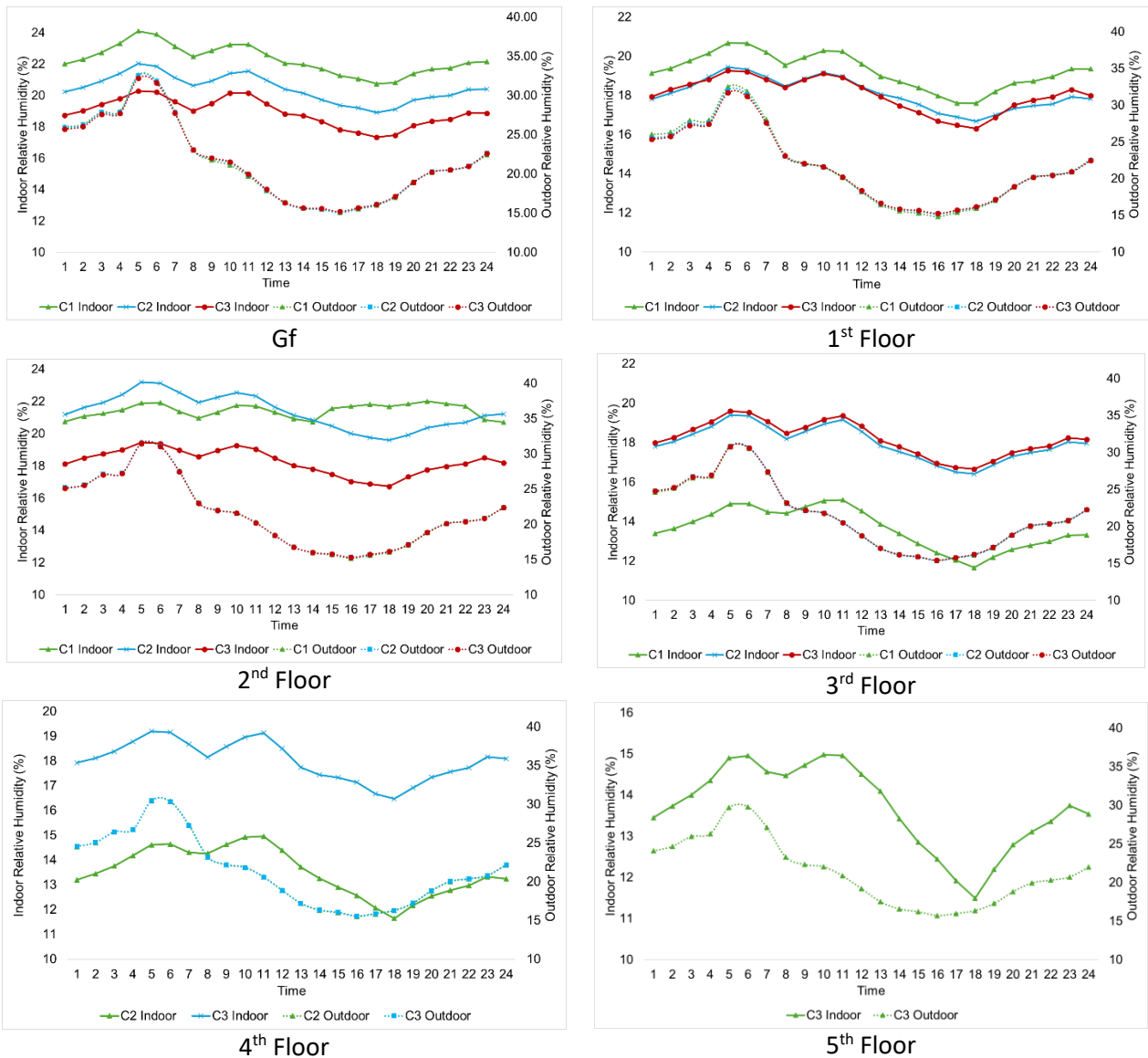
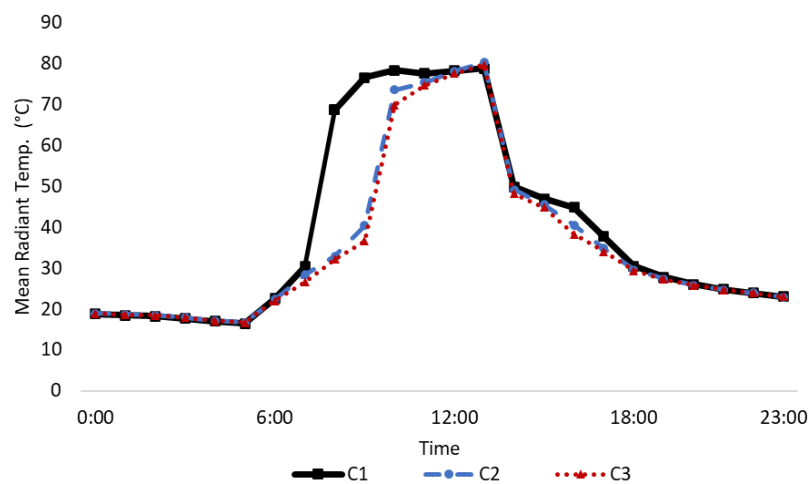


Figure 9. Examine the Relative Humidity trends throughout the day across various cases.

### Analysis of Mean Radiant Temperature *Tmrt*

The study describes the *Tmrt* values obtained from the different cases: C1, C2, and C3. The mean radiant temperature ranges and average values for each case are provided. The *Tmrt* value experienced an increase from 6:00 a.m. to 6:00 p.m. across all cases. This rise can be attributed to the elevated position of the sun during the summer solstice, coupled with the intense and prolonged duration of solar radiation. Results indicate variations in *Tmrt* values among the cases. Between 6:00 a.m. and 12:00 p.m., all three cases exhibit a marked increase in temperature, peaking at 80°C. After noon, temperatures decline for all three cases. At the beginning and end of the day, the temperatures for all three cases converge at approximately 20°C. The behavior of the three cases is very similar overall; however, the difference between them becomes more pronounced as C1's temperature rises from 7:00 a.m. to 12:00 p.m., while the behavior of C2 and C3 remains close during this period. C1

shows the widest  $T_{mrt}$  range, ranging from 16.50°C to 78.82°C, and the highest average  $T_{mrt}$  value of 40.32°C. This indicates that C1 experiences slightly higher radiative temperatures on average compared to C2 and C3. On the other hand, C2 has a slightly narrower temperature range, ranging from 16.70°C to 80.19°C, and a lower average  $T_{mrt}$  value of 36.93°C. This means that C2 generally experiences lower radiative temperatures compared to C1, but higher temperatures compared to C3. The C3 temperature ranges from 16.69 °C to 79.66 °C and the lowest average  $T_{mrt}$  value of 36.23 °C among the three cases. This indicates that C3 experiences the lowest radiant temperatures on average, as shown in Figure 10. These findings are significant as the aspect ratio inversely affects  $T_{mrt}$  due to higher buildings casting longer shadows, thereby diminishing direct solar radiation. Additionally, the diminished sky view factor lowers exposure to cooler skies, impeding radiant energy. Elevated aspect ratios impede radiative heat exchange, while factors such as thermal mass and the urban heat island phenomenon further contribute to the reduction in  $T_{mrt}$  [51-54].



**Figure 10. Results of  $T_{mrt}$  for processed cases**

### The Effect of Proposed Cases on the PET

As previously mentioned, PET has emerged as a highly suitable indicator for quantifying thermal comfort levels in outdoor environments and investigating the variations in the PET index in different cases investigated. To accomplish this, Data collected throughout the day using the ENVI-met and Rayman software tools were utilized to compare the output results. PET exhibited a rise from 6:00 a.m. to 6:00 p.m., with the peak value consistently recorded at 1:00 p.m. across all instances. The higher PET values during the daytime are attributed to the exposure to solar radiation. In C1, the PET values ranged from 21.60 °C to 61.70 °C, with an average PET value of 38.24 °C. Moving on to C2, the PET values ranged from 21.80 °C to 62.50 °C, with an average PET value of 36.53 °C. Lastly, in C3, the PET values ranged from 21.90 °C to 62.20 °C, with an average PET value of 36.18 °C, as depicted in Figure 11. All cases begin with PET values between 10 and 20°C, indicating conditions ranging from moderately cold to rest until 6:00 a.m. Between 6:00 a.m. and 12:00 p.m., PET values increase sharply, reaching a peak around 65 °C for the C1 case, indicating strong to intense heat, while C2 and C3 remain close together with peaks around 60 °C. After noon, values begin to gradually decline back to around 20°C by the end of the day, again reflecting comfortable conditions. It is observed that the behavior of C1 shows a faster and larger temperature rise compared to C2 and C3 but follows the same general trend of afternoon decrease. These findings indicate that an increase in the aspect ratio

leads to a reduction in PET values. This relationship is attributed to the taller buildings casting larger shadows, resulting in a greater shaded area. Consequently, this phenomenon contributes to an enhancement of thermal comfort within the vicinity [51].

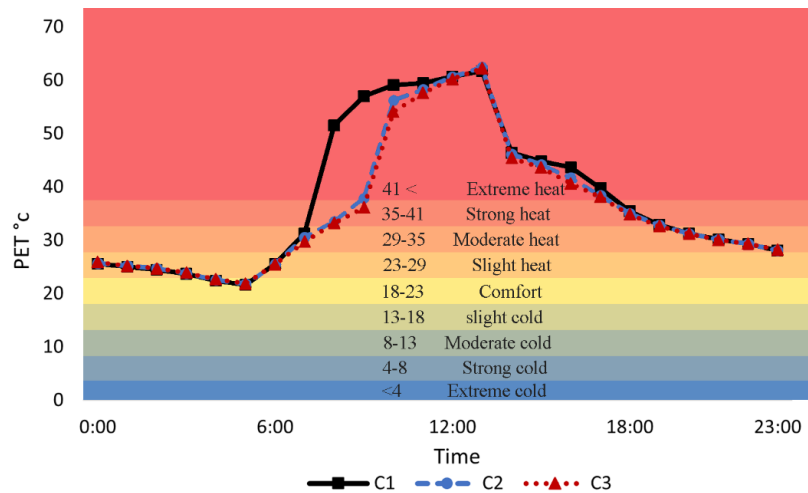


**Figure 11. Results of PET for processed cases**

### Assessing the internal thermal conditions and associate energy

#### *Thermal comfort for the investigated building*

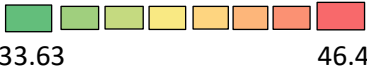
Table 8 presents the operative temperature values for various floors and proposed cases (C1, C2, and C3). The temperatures vary across floors and cases, showing a trend of increasing operative temperatures on higher floors. On the GF, the temperatures are relatively stable across all three cases, with C1 showing a minimum temperature of 35.66°C, a maximum of 38.22°C, and an average of 37.00°C. C2 has nearly identical values, while C3 shows slightly higher values, with an average of 37.43°C, suggesting a marginal increase in thermal load. Moving to the 1st floor, there is a moderate rise in operative temperatures, especially in Cases C2 and C3, where averages reach 38.13°C and 38.10°C, respectively. C1 remains the most stable with an average of 37.01°C. On the 2nd floor, significant variation occurs, particularly in C2, which exhibits the lowest values across all floors, with a minimum of 33.63°C and an average of 35.17°C, indicating improved thermal performance. In contrast, C1 records higher temperatures with an average of 38.37°C, while C3 follows closely at 38.02°C. The 3rd floor experiences a sharp increase in temperatures, particularly in C1, where the average temperature rises to 43.83°C, reflecting a considerable deterioration in thermal comfort. In contrast, Cases C2 and C3 maintain significantly lower averages of 38.28°C and 38.03°C, respectively, suggesting better thermal regulation. On the 4th floor, the trend continues with C2 showing high temperatures, averaging 43.87°C, while C3 maintains a lower average of 38.22°C. Finally, on the 5th floor, C3 records its highest values, with an average of 43.68°C, highlighting the increased thermal discomfort on upper floors due to higher solar exposure and reduced cooling efficiency, as depicted in Figure 12. These variations across cases and floors suggest that design and operational modifications significantly influence thermal comfort, with C2 performing better on certain floors, particularly the second floor. At the same time, C1 consistently shows higher temperatures on the upper levels. The observed increase in operative temperature values with floor height suggests that internal thermal conditions worsen as one ascends through the building, potentially leading to discomfort. This trend can be attributed to several factors, such as increased exposure to direct solar

radiation on higher floors, which leads to higher heat gains. Additionally, the effectiveness of passive cooling strategies, such as natural ventilation or shading, may diminish on upper levels, exacerbating temperature increases. Furthermore, the performance of HVAC systems may vary, with the upper floors experiencing greater difficulty maintaining consistent cooling due to factors like heat stratification or reduced system efficiency at those heights.

### **Analysis of Cooling Energy Consumption**

Figure 13 presents an analysis designed to identify patterns and relationships between floor levels, cooling requirements, and the impact of different aspect ratios on energy consumption, with a focus on the energy consumption of the residential unit across different floors. As presented in Figure (12), energy consumption for the GF increases progressively with higher ratios. Specifically, energy consumption starts at 15,428.88 kWh for an aspect ratio of 1.5 (C1) and reaches 16,857.97 kWh at an aspect ratio of 2.25 (C3). In contrast, the 1st floor exhibits a different trend. Energy consumption peaks at an aspect ratio of 1.87 (C2) with a value of 19,685.34 kWh, before decreasing to 17,688.34 kWh at an aspect ratio of 2.25 (C3). 2nd floor shows relatively stable energy usage across all three aspect ratios, with values of 18,374.87 kWh (C1), 18,070.75 kWh (C2), and 18,286.65 kWh (C3), indicating minor fluctuations.

**Table 8.** Operative Temperature Analysis Across Different Floors and Proposed Cases

Floors	Proposed cases	Operative Temperature		
		Min	Max	Av.
GF	C1	35.66	38.22	37.00
	C2	35.65	38.20	36.98
	C3	36.05	38.75	37.43
1st	C1	35.43	38.39	37.01
	C2	36.60	39.42	38.13
	C3	36.61	39.37	38.10
2 <sup>nd</sup>	C1	36.76	39.82	38.37
	C2	33.63	36.50	35.17
	C3	36.53	39.28	38.02
3 <sup>rd</sup>	C1	41.65	46.35	43.83
	C2	36.71	39.70	38.28
	C3	36.56	39.31	38.03
4 <sup>th</sup>	C2	41.71	46.39	43.87
	C3	36.67	39.62	38.22
5 <sup>th</sup>	C3	41.57	46.15	43.68
				

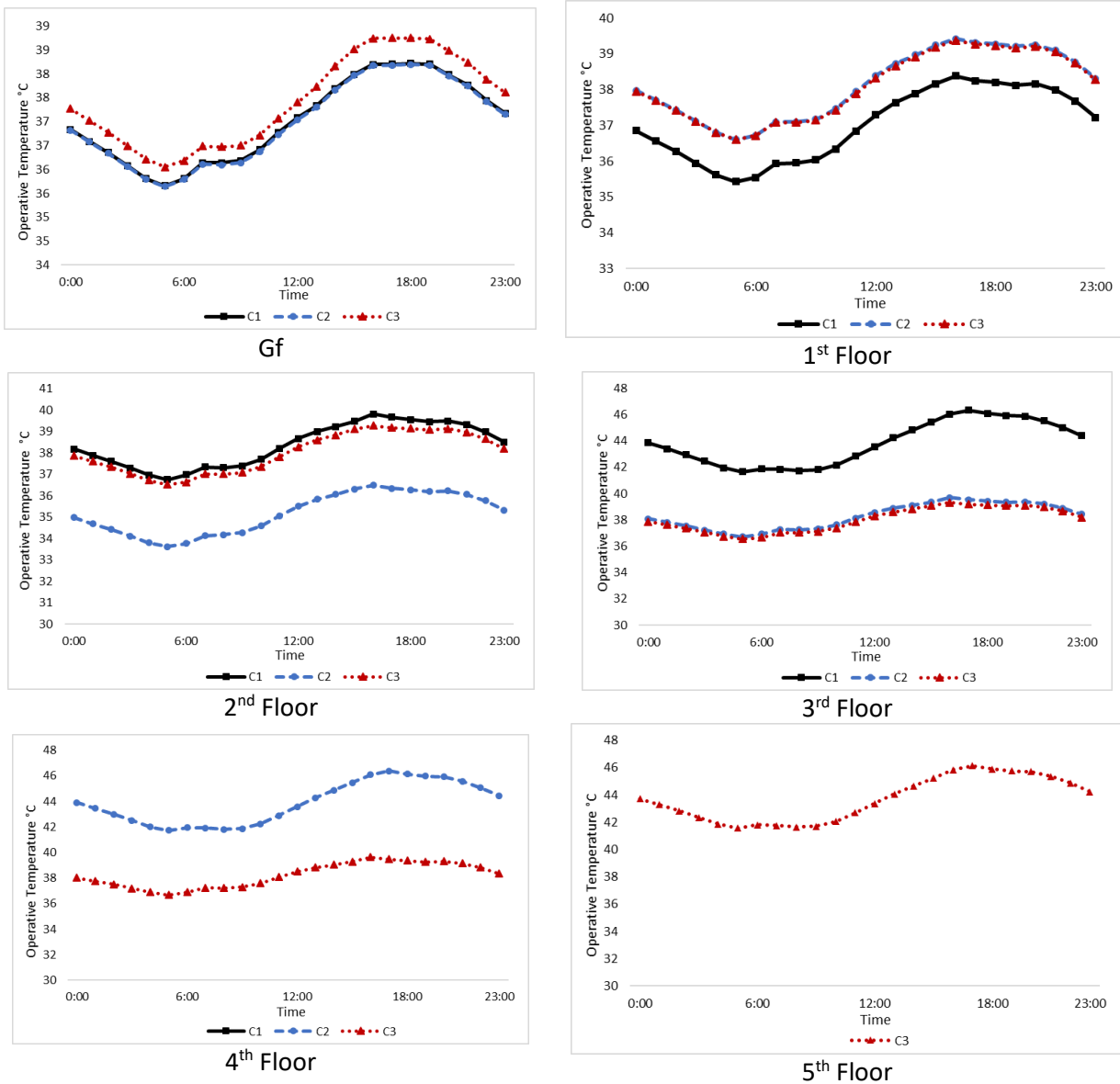


Figure 12. Examine the Operative Temperature trends throughout the day across various cases.

The 3rd floor presents significant variation in energy consumption. The highest value is observed at an aspect ratio of 1.5 (C1), with 29,396.92 kWh. This consumption then drops considerably to higher aspect ratios, with values of 17,248.86 kWh (C2) and 18,067.39 kWh (C3). 4th floor, the data is incomplete for aspect ratio 1.5 (C1). However, the available data shows an increase in energy consumption from 29,441.22 kWh at an aspect ratio of 1.87 (C2) to 18,208.33 kWh at an aspect ratio of 2.25 (C3). Finally, the 5th floor only has data for aspect ratio 2.25 (C3), with a recorded value of 29,304.14 kWh. This value is comparable to the lower energy consumption levels observed on other floors at the same ratio.

To interpret these results, the study categorizes the floor levels into three main tiers. The GF, representing the lower level, shows that the rear setback aspect ratio has a significant effect on energy consumption. Specifically, higher aspect ratios are associated with increased cooling demands. This trend can be attributed to the solar altitude angle at solar noon in Aswan during July, which is approximately 89.5 degrees. This angle results in significant heat accumulation without adequate dissipation due to limited airflow at the base of the rear setback, particularly at elevated aspect ratios. In the middle floors, energy consumption increases with a small rear setback aspect

ratio and decreases with a higher aspect ratio for several reasons. Small rear setback ratios limit vertical space, restricting airflow and reducing natural ventilation. This restriction leads to higher indoor temperatures due to increased heat accumulation, necessitating more energy for cooling systems to maintain comfortable conditions, thereby resulting in higher energy consumption.

Conversely, a higher rear setback aspect ratio enhances airflow and natural ventilation, facilitating heat dissipation. The increased vertical space allows hot air to rise and escape, creating a cooler environment in the middle floors. Consequently, cooling systems require less energy to maintain comfortable temperatures, leading to reduced energy consumption. In contrast, the upper floors experience heightened exposure to direct solar radiation, resulting in increased energy requirements for cooling. This exposure highlights the importance of implementing strategies to mitigate solar gain in upper-level spaces to optimize energy efficiency in cooling systems.

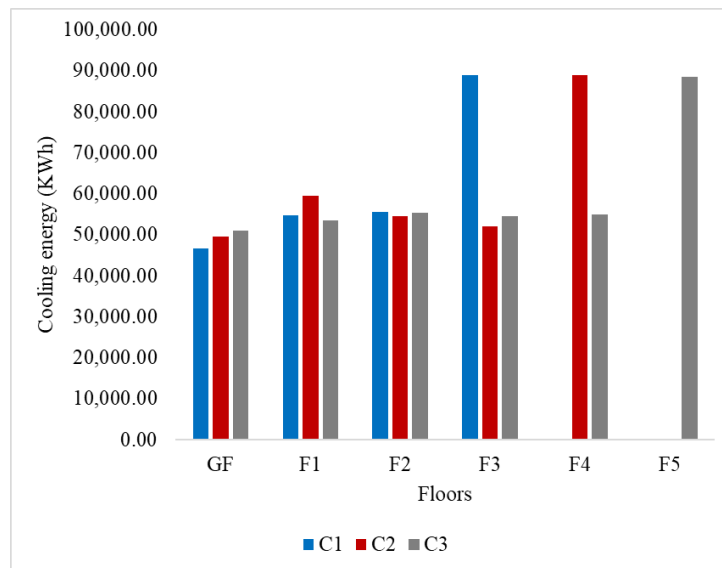


**Figure 13.** Analysis of Cooling Energy Consumption

### ***Analysis of the Relationship Between Aspect Ratios and Energy Performance***

As illustrated in Figure 13, the analysis of the relationship between aspect ratios and energy performance metrics across various scenarios highlights a strong linear correlation. This correlation is particularly pronounced in the case of the lower floors, where the aspect ratio emerges as a critical factor influencing energy consumption. The analysis of the relationship on the fifth floor is influenced by the absence of comparable floors in the other cases and their termination. The data reveals a coefficient of determination ( $R^2$ ) value of 0.88, indicating that 88% of the variations in energy consumption can be attributed to changes in the aspect ratio. Such a high  $R^2$  value is a strong indicator of the predictive strength of the aspect ratio in determining energy efficiency outcomes. As the aspect ratio adjusts, there is a corresponding and predictable impact on energy usage. This linearity emphasizes that the geometric proportions of a building—represented by its aspect ratio—play a pivotal role in shaping its energy performance. For lower floors, this relationship might be influenced by specific factors such as exposure to external environmental conditions (e.g., sunlight, wind, and shading), ventilation dynamics, and thermal heat gains or losses. These factors are more pronounced on lower floors due to proximity to ground-level thermal mass, urban heat effects, and interaction with surrounding structures or landscaping. The strong linear correlation shown in the

data underscores the importance of considering aspect ratio as a fundamental design parameter during the early stages of building planning.

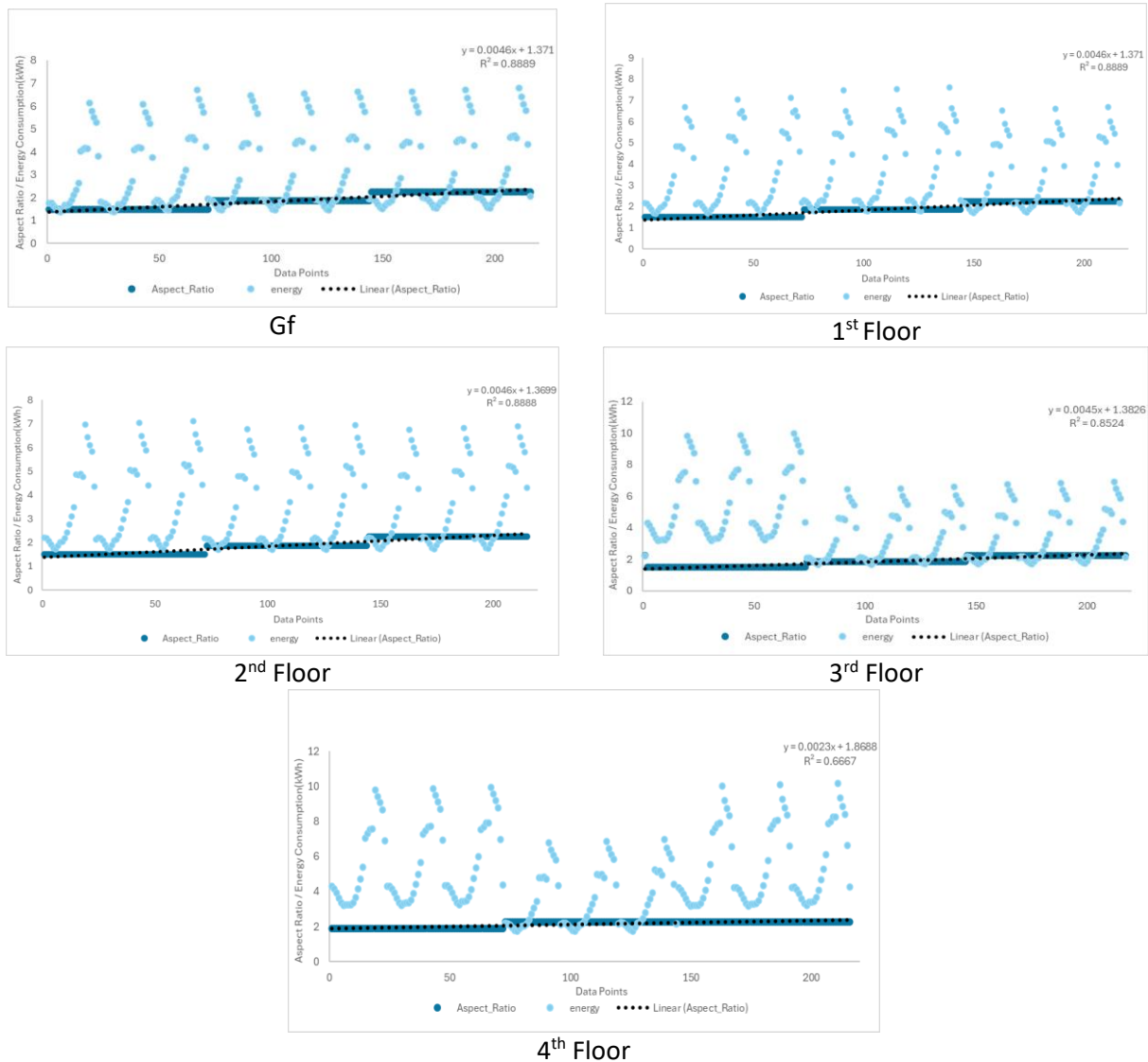


**Figure 13. Examine relationships between aspect ratios and energy performance metrics, across various cases.**

### Conclusions

The study addresses improving external and internal thermal comfort and energy efficiency in buildings near setback areas, especially in hot arid climates such as Aswan. As the study mentioned, despite the research on street dimensions and thermal comfort, there is a gap regarding setback areas and their impact on interior comfort. Despite the regular shape of the setback area adherence to the building law during the case studies, changes in aspect ratio were observed to impact external thermal conditions, which in turn affect indoor thermal comfort and energy efficiency in adjacent spaces. The aspect ratio impacts different building floors in varying ways across the three cases studied. As the aspect ratio increases, thermal conditions improve on the middle floors. In contrast, the lower floors experience higher temperatures due to greater heat retention from ground radiation, heat accumulation, and reduced airflow. This effect is especially pronounced in Aswan’s hot climate, where the sun’s angle is high. Therefore, insulation methods must be considered throughout the lower floors of the building, and a combination of solar design and thermal design

strategies should be implemented, rather than relying solely on solar design. The findings of the study can be generally discussed concerning two key issues: the microclimate created by rear setbacks and the energy dynamics in adjacent buildings, as follows:

- A consistent trend was observed in which  $T_a$  increased, and RH decreased with elevation. The second floor of the C2 case exhibited the most favorable internal thermal conditions, with the lowest temperature differences ( $\Delta T$ ) between indoor and outdoor environments. This suggests that the aspect ratio in C2 enhances insulation and shading effects through this floor, improving thermal comfort.
- As for energy efficiency, increasing the rear setback ratio affects energy consumption differently depending on the floor level. In the lower floors, energy consumption increases with a higher setback ratio due to heat accumulation and reduced airflow when the sun's angle is high. In contrast, the middle floors benefit from the increased setback ratio, which enhances natural ventilation and reduces temperatures, thereby lowering energy demand. As for the upper floors, they experience greater exposure to direct sunlight, which increases energy consumption for cooling, highlighting the importance of strategies to reduce heat gain on those floors.

The study underscores the importance of setback design in enhancing thermal comfort and energy efficiency in buildings, particularly in hot arid climates like Aswan. It reveals that setback aspect ratios significantly impact thermal conditions across different floor levels, affecting indoor comfort and energy consumption. The findings advocate for an integrated design approach that combines solar and thermal strategies, including adaptive HVAC systems, insulation, and natural ventilation, tailored to specific floor conditions. To validate these findings, a comparison with previous studies reveals consistency in several aspects. Research on urban canyons and street dimensions also supports the observation that increased aspect ratios enhance ventilation and shading effects, thereby improving thermal comfort in middle-level spaces. Similarly, studies in hot-arid climates, such as Riyadh and Dubai, confirm that lower floors often face significant heat retention challenges due to ground radiation and limited airflow [4, 55-60]. These comparative insights reinforce the reliability of this study's outcomes. The research highlights the need for climate-responsive building regulations, urban planning considerations to reduce heat stress, and retrofitting strategies for existing structures. This holistic approach can guide sustainable development in similar hot climates, optimizing thermal environments and reducing energy use. Future work could focus on optimizing the decision-making process to assist stakeholders in selecting the most effective solutions regarding the aspect ratios of rear setbacks and window-to-wall ratios.

## References

1. Abdeen Mustafa Omer, "Energy, environment and sustainable development," *Renewable and sustainable energy reviews*, vol. 12, no. 9, pp. 2265-2300, 2008.
2. Dalia Tarek, Marwa El-Naggar, Hesham Sameh, Ayman Yousef, and Ayman Ragab, "Energy Efficiency Coupled with Lightweight Bricks: Towards Sustainable Building: A review," *SVU-International Journal of Engineering Sciences and Applications*, vol. 4, no. 1, pp. 1-28, 2023.

3. Lars Carlsen and Rainer Bruggemann, "The 17 United Nations' sustainable development goals: A status by 2020," *International Journal of Sustainable Development & World Ecology*, vol. 29, no. 3, pp. 219-229, 2022.
4. Abdelaziz Farouk Mohamed, Amira Ahmed Amir, and Ayman Ragab, "The effect of aerogel glazing on daylight and heat gain in school buildings in hot and dry climate," *Environment, Development and Sustainability*, pp. 1-22, 2024.
5. Sama Ahmed, Mohamed Esmat El Attar, Nasser Zouli, Ahmed Abutaleb, Ibrahim M Maafa, MM Ahmed, . . . Ayman Ragab, "Improving the thermal performance and energy efficiency of buildings by incorporating biomass waste into clay bricks," *Materials*, vol. 16, no. 7, p. 2893, 2023.
6. Hatem Mahmoud and Ayman Ragab, "Thermal Performance Evaluation of Unshaded Courtyards in Egyptian Arid Regions," *Smart and Sustainable Planning for Cities and Regions: Results of SSPCR 2019 3*, pp. 109-121, 2021.
7. MOHAMMAD Fahmy, "Climate change adaptation for mid-latitude urban developments," in *PLEA2012-28th Conference, opportunities, limits & needs towards an environmentally responsible architecture*, 2012, pp. 7-9.
8. Rania E Ashmawy and NY Azmy, "Buildings orientation and its impact on the energy consumption," 2018.
9. Zohreh Shaghaghian, Fatemeh Shahsavari, and Elham Delzende, "Studying Buildings Outlines to Assess and Predict Energy Performance in Buildings: A Probabilistic Approach," *arXiv preprint arXiv:2111.08844*, 2021.
10. Mohamed Ahmed Alaa El Din Ahmed and Mohamed Anwar Fikry, "Impact of glass facades on internal environment of buildings in hot arid zone," *Alexandria Engineering Journal*, vol. 58, no. 3, pp. 1063-1075, 2019.
11. Albert Al Touma and Djamel Ouahrani, "Shading and day-lighting controls energy savings in offices with fully-Glazed façades in hot climates," *Energy and Buildings*, vol. 151, pp. 263-274, 2017.
12. Abdelmonteleb Mohammed Aly, Mohammed Hassan Hassn, Yman Ragab Abdel Rady, and Alia Tarek Mohammed, "The effect of using nano-materials in external openings on energy consumption in hot desert climate," *JES. Journal of Engineering Sciences*, vol. 48, no. 3, pp. 468-477, 2020.
13. Ayman Ragab and Ahmed Abdelrady, "Impact of green roofs on energy demand for cooling in Egyptian buildings," *Sustainability*, vol. 12, no. 14, p. 5729, 2020.
14. Mohamed Hssan Hassan Abdelhafez, Ali Abdulmohsen Aldersoni, Mohammad Mansour Gomaa, Emad Noaime, Mohammed Mashary Alnaim, Mohammed Alghaseb, and Ayman Ragab, "Investigating the thermal and energy performance of advanced glazing systems in the context of Hail City, KSA," *Buildings*, vol. 13, no. 3, p. 752, 2023.
15. Badia Ghassan Masoud, Isabel Crespo Cabillo, Helena Coch Roura, and Benoit Beckers, "Effects of urban morphology on shading for pedestrians: sky view factor (SVF) as an indicator of solar access," in *PLEA 2018: Smart and Healthy Within the Two-Degree Limit: proceedings of the 34th International Conference on Passive and Low Energy Architecture: Dec 10-12, 2018 Hong Kong, China*, 2019, pp. 1029-1030.
16. Ibrahim Rizk Hegazy and Emad Mohammed Qurnfulah, "Thermal comfort of urban spaces using simulation tools exploring street orientation influence of on the outdoor thermal comfort: a case study of Jeddah, Saudi Arabia," *International Journal of Low-Carbon Technologies*, vol. 15, no. 4, pp. 594-606, 2020.
17. M Mahgoub, N Hamza, and S Dudek, "Shading Historical Commercial Streets in Hot Arid Areas: Questioning the Common Wisdom," in *33rd International Conference Passive Low Energy Architecture PLEA 2017*. 2017, 2017: Newcastle University.

18. Omnia Fawzy Abdulsalam and Ahmed Haleem Hussien, "Implications of urban space aspect ratio on campus outdoor thermal comfort (Case study, BUE campus, Cairo, Egypt)," *Engineering Research Journal*, vol. 170, pp. 1-10, 2021.
19. Khaled Elkhayat, Mohamed Hssan Hassan Abdelhafez, Fatmaelzhraa Altaf, Steve Sharples, Mohammad A. Alshenaifi, Sultan Alfraidi, . . . Ayman Ragab, "Urban geometry as a climate adaptation strategy for enhancing outdoor thermal comfort in a hot desert climate," *Frontiers of Architectural Research*, 2024/10/16/ 2024.
20. Hatem Mahmoud and Ayman Ragab, "Urban geometry optimization to mitigate climate change: towards energy-efficient buildings," *Sustainability*, vol. 13, no. 1, p. 27, 2020.
21. Tetsu Kubota and Doris Hooi Chyee Toe, "Application of passive cooling techniques in vernacular houses to modern urban houses: A case study of Malaysia," *Procedia-Social and Behavioral Sciences*, vol. 179, pp. 29-39, 2015.
22. Naja Aqilah, Hom Bahadur Rijal, and Sheikh Ahmad Zaki, "A review of thermal comfort in residential buildings: Comfort threads and energy saving potential," *Energies*, vol. 15, no. 23, p. 9012, 2022.
23. Danijela Kuzmanović, Gregor Skok, and Jana Banko, "Improving the operational forecasts of outdoor UTCI with post-processing," *Copernicus Meetings2023*.
24. Leonardo Marques Monteiro and MARCIA PEINADO Alucci, "An outdoor thermal comfort index for the subtropics," *Proceeding 26th PLEA*, 2009.
25. Michael A Humphreys and J Fergus Nicol, "The validity of ISO-PMV for predicting comfort votes in everyday thermal environments," *Energy and buildings*, vol. 34, no. 6, pp. 667-684, 2002.
26. Mohammad Kazkaz and Milan Pavelek, "Operative temperature and globe temperature," *Eng. Mech*, vol. 20, no. 3/4, pp. 319-325, 2013.
27. Reem Abd Elraouf, Ashraf Elmokadem, Naglaa Megahed, Osama Abo Eleinen, and Sara Eltarabily, "The impact of urban geometry on outdoor thermal comfort in a hot-humid climate," *Building and Environment*, vol. 225, p. 109632, 2022.
28. Khalid Setaih, "The effect of asymmetrical street aspect ratios on urban wind flow and pedestrian thermal comfort conditions," *Newcastle University*, 2016.
29. Nazanin Nasrollahi, Yasaman Namazi, and Mohammad Taleghani, "The effect of urban shading and canyon geometry on outdoor thermal comfort in hot climates: A case study of Ahvaz, Iran," *Sustainable Cities and Society*, vol. 65, p. 102638, 2021.
30. Nastaran Abdollahzadeh and Nimish Boloria, "Outdoor thermal comfort: Analyzing the impact of urban configurations on the thermal performance of street canyons in the humid subtropical climate of Sydney," *Frontiers of Architectural Research*, vol. 10, no. 2, pp. 394-409, 2021.
31. Mohammed A Bakarman and Jae D Chang, "The influence of height/width ratio on urban heat island in hot-arid climates," *Procedia Engineering*, vol. 118, pp. 101-108, 2015.
32. Alaoui Sosse Jihad and Mohamed Tahiri, "Modeling the urban geometry influence on outdoor thermal comfort in the case of Moroccan microclimate," *Urban Climate*, vol. 16, pp. 25-42, 2016.
33. Fazia Ali-Toudert and Helmut Mayer, "Numerical study on the effects of aspect ratio and orientation of an urban street canyon on outdoor thermal comfort in hot and dry climate," *Building and environment*, vol. 41, no. 2, pp. 94-108, 2006.
34. Peng Cui, Jinjian Jiang, Jie Zhang, and Lei Wang, "Effect of street design on UHI and energy consumption based on vegetation and street aspect ratio: Taking Harbin as an example," *Sustainable Cities and Society*, vol. 92, p. 104484, 2023.

35. Jifa Rao, Bohong Zheng, and Jiayu Li, "Exploring the Effect of Aspect Ratio (H/W) on Thermal Environment in Multiple Climate Zones with Open-Source Data," *Buildings*, vol. 14, no. 2, p. 342, 2024.
36. Rana Elbadri, Hassan Abdel-Salam, and Mohamed Fikry, "Airflow in Urban Environment: an Approach to Improve Egyptian Buildings Regulations," in *LET IT GROW, LET US PLAN, LET IT GROW. Nature-based Solutions for Sustainable Resilient Smart Green and Blue Cities. Proceedings of REAL CORP 2023, 28th International Conference on Urban Development, Regional Planning and Information Society, 2023*, pp. 25-35: CORP–Competence Center of Urban and Regional Planning.
37. Taihan Chen, Hongyu Yang, Guanwen Chen, Cho Kwong Charlie Lam, Jian Hang, Xuemei Wang, Hong Ling, "Integrated impacts of tree planting and aspect ratios on thermal environment in street canyons by scaled outdoor experiments," *Science of The Total Environment*, vol. 764, p. 142920, 2021.
38. Rizwan Ahmed Memon, ABDUL HAQUE Tunio, and KANYA Lal, "Impact of Aspect Ratio and Solar Heating on Street Canyon Air Temperatures," *Mehran University Research Journal of Engineering and Technology*, vol. 30, no. 1, pp. 105-116, 2011.
39. Peter J Crank, David J Sailor, George Ban-Weiss, and Mohammad Taleghani, "Evaluating the ENVI-met microscale model for suitability in analysis of targeted urban heat mitigation strategies," *Urban climate*, vol. 26, pp. 188-197, 2018.
40. Aisyah Nabilah, Lukman Noor Hakim, Maulana Calvin Fawzy, and Try Ramadhan, "Outdoor Thermal Comfort: Application of RayMan Tools," in *IOP Conference Series: Earth and Environmental Science*, 2021, vol. 738, no. 1, p. 012008: IOP Publishing.
41. Daniel Mann, Cindy Yeung, Roberto Habets, Zeger Vroon, and Pascal Buskens, "Comparative building energy simulation study of static and thermochromically adaptive energy-efficient glazing in various climate regions," *Energies*, vol. 13, no. 11, p. 2842, 2020.
42. Capterra. C DesignBuilder Reviews. [Online]. Available: <https://www.capterra.com/p/130062/DesignBuilder/reviews/>
43. Andreas Matzarakis, Frank Rutz, and Helmut %J International journal of biometeorology Mayer, "Modelling radiation fluxes in simple and complex environments: basics of the RayMan model," vol. 54, no. 2, pp. 131-139, 2010.
44. Tzu-Ping Lin, Andreas Matzarakis, Ruey-Lung %J Building Hwang, and environment, "Shading effect on long-term outdoor thermal comfort," vol. 45, no. 1, pp. 213-221, 2010.
45. Kuo-Tsang Huang, Shing-Ru Yang, Andreas Matzarakis, and Tzu-Ping Lin, "Identifying outdoor thermal risk areas and evaluation of future thermal comfort concerning shading orientation in a traditional settlement," *Science of the Total Environment*, vol. 626, pp. 567-580, 2018.
46. Hatem Mahmoud and Ayman Ragab, "Impact of urban geometry on cooling loads in Egypt: Case study: A social residential compound in New Aswan city," in *2020 9th International Conference on Power Science and Engineering (ICPSE), 2020*, pp. 71-75: IEEE.
47. Ayman Ragab Abdelrady Mahmoud, Abdelmonteleb Mohammed Aly, and Mohammed Hassaan Hassan, "Evaluating the thermal performance of urban spaces in aswan city "a case study of saad zaghoul street," *JES. Journal of Engineering Sciences*, vol. 43, no. 5, pp. 766-782, 2015.
48. Mohamed Gomaa and Ayman Ragab, "Investigating the Spatial Autocorrelation of Surface-Air Temperature for Different Ground Materials in Hot Desert Climate," *The Egyptian International Journal of Engineering Sciences and Technology*, vol. 39, no. 1, pp. 49-59, 2022.
49. Ayman Ragab, Nasser Zouli, Ahmed Abutaleb, Ibrahim M Maafa, MM Ahmed, and Ayman Yousef, "Environmental and economic benefits of using pomegranate peel waste for insulation bricks," *Materials*, vol. 16, no. 15, p. 5372, 2023.

50. Dongsu Kim, Heejin Cho, Im, and Piljae Sam Cox, "Modeling and Calibration of a Variable Refrigerant Flow (VRF) System with a Dedicated Outdoor Air System (DOAS)," in *Building Simulation 2017*, 2017, vol. 15, pp. 1456-1462: IBPSA.
51. José Rodríguez-Algeciras, Abel Tablada, Mabel Chaos-Yeras, Guillermo De la Paz, and Andreas Matzarakis, "Influence of aspect ratio and orientation on large courtyard thermal conditions in the historical centre of Camagüey-Cuba," *Renewable energy*, vol. 125, pp. 840-856, 2018.
52. Chahrazed Kedissa, Saliha Outtas, and Rafik Belarbi, "The impact of height/width ratio on the microclimate and thermal comfort levels of urban courtyards," *International Journal of Sustainable Building Technology and Urban Development*, vol. 7, no. 3-4, pp. 174-183, 2016.
53. Qun Dai and Marc Aurel Schnabel, "Thermal comfort levels classified by aspect ratio and orientation for three zones of a street in Rotterdam," *Architectural Science Review*, vol. 57, no. 4, pp. 286-294, 2014.
54. Beta Paramita and Hiroatsu Fukuda, "Study on The Affect of Aspect Building Form and Layout," 2012.
55. Sundus Luay Shareef, "Urban Geometry: The Effect of Height Diversity and Buildings Configuration on Thermal Performance and Cooling Load at Urban Scale. A Case Study in Dubai/UAE," *The British University in Dubai*, 2018.
56. Badran Masoud Alznafer, "The impact of neighbourhood geometries on outdoor thermal comfort and energy consumption from urban dwellings: a case study of the Riyadh city, the kingdom of Saudi Arabia," *Cardiff University*, 2014.
57. Omar Almahdy, "Making a Hot, Arid, Desert Arab City More Livable: Investigating the Role of Street Design in Enhancing Walkability in Riyadh, Saudi Arabia," *Illinois Institute of Technology*, 2020.
58. Arid Climates, "The Effect of Urban Geometry on the Microclimate in Hot."
59. MHH Abdelhafez, "Green residential districts in hot desert climate towards low energy consumption," *Journal of Engineering and Applied Science*, vol. 65, no. 1, pp. 1-21, 2018.
60. Mai Mostafa Hassieb, Ayman Ragab, and Abdelaziz Farouk Mohamed, "Quantifying the Influence of Window-to-Wall Ratio (WWR) on Indoor Air Quality and Thermal Comfort: Classroom Study in Hot Arid Climates," in *IOP Conference Series: Earth and Environmental Science*, 2024, vol. 1396, no. 1, p. 012025: IOP Publishing.